

UNIVERSIDAD SAN FRANCISCO DE QUITO USFQ

Colegio de Ciencias Biológicas y Ambientales

**Filogeografía y Genética de Poblaciones de Rayas Águila en el
Pacífico Oriental Tropical**

Mateo Vinueza Guarderas

Biología

Trabajo de fin de carrera presentado como requisito
para la obtención del título de
Biólogo

Quito, 18 de diciembre de 2024

UNIVERSIDAD SAN FRANCISCO DE QUITO USFQ

Colegio de Ciencias Biológicas y Ambientales

**HOJA DE CALIFICACIÓN
DE TRABAJO DE FIN DE CARRERA**

Filogeografía y Genética de Poblaciones de Rayas Águila en el Pacífico Oriental Tropical

Mateo Vinueza Guarderas

Nombre del profesor, Título académico Diana Pazmiño PhD y María José Pozo MBS

Quito, 18 de diciembre de 2024

© DERECHOS DE AUTOR

Por medio del presente documento certifico que he leído todas las Políticas y Manuales de la Universidad San Francisco de Quito USFQ, incluyendo la Política de Propiedad Intelectual USFQ, y estoy de acuerdo con su contenido, por lo que los derechos de propiedad intelectual del presente trabajo quedan sujetos a lo dispuesto en esas Políticas.

Asimismo, autorizo a la USFQ para que realice la digitalización y publicación de este trabajo en el repositorio virtual, de conformidad a lo dispuesto en la Ley Orgánica de Educación Superior del Ecuador.

Nombres y apellidos.	Mateo Vinueza Guarderas
Código:	00211787
Cédula de identidad:	1721104485
Lugar y fecha:	Quito, 18 de diciembre de 2024

ACLARACIÓN PARA PUBLICACIÓN

Nota: El presente trabajo, en su totalidad o cualquiera de sus partes, no debe ser considerado como una publicación, incluso a pesar de estar disponible sin restricciones a través de un repositorio institucional. Esta declaración se alinea con las prácticas y recomendaciones presentadas por el Committee on Publication Ethics COPE descritas por Barbour et al. (2017) Discussion document on best practice for issues around theses publishing, disponible en <http://bit.ly/COPETHeses>.

UNPUBLISHED DOCUMENT

Note: The following capstone project is available through Universidad San Francisco de Quito USFQ institutional repository. Nonetheless, this project – in whole or in part – should not be considered a publication. This statement follows the recommendations presented by the Committee on Publication Ethics COPE described by Barbour et al. (2017) Discussion document on best practice for issues around theses publishing available on <http://bit.ly/COPETHeses>.

ABSTRACT

The Eastern Tropical Pacific (ETP) Spotted Eagle Ray *Aetobatus laticeps*, is a is an understudied species with limited ecological and conservation information. Only in the last 10 years these rays were redescribed as distinct species from a formerly widespread species complex *Aetobatus narinari* (ANSC). However, the sampling of the studies that divided the ANSC was not geographically balanced, with most of the individuals (50) being collected in the Atlantic while only (5) were taken from the ETP. Given this region's vast extension and environmental heterogeneity, it's possible that it's obscuring a large proportion of the genetic variation of the genus as a whole and possibly the presence of new species. Because eagle rays have relatively low fecundity, and are subject to directed and incidental fisheries, they are highly susceptible to population declines. Consequently, elucidating the species diversity, their distribution range, and their internal genetic variability and interconnectivity is crucial to correctly assess their conservation status. Through a mixed genetic marker approach, we assessed ETP eagle ray's phylogeny, genetic diversity and phylogeography. First, we found that eagle rays in this region correspond to *Aetobatus laticeps*. Second, we found alarmingly low levels of genetic variability across all markers, while simultaneously showing a high degree of geographic-genetic structuring. Finally, our data pointed to three possible mechanisms that could explain the population structuring we encountered: A) Isolation by distance B) Isolation by philopatry, and C) Isolation by depth. To this date, this is the first and only study to meaningfully assess eagle rays genetic diversity in the Eastern Tropical Pacific, shedding light into a species that has been understudied and ignored for far too long. Pointing to this species increased susceptibility to both direct and by-catch fishing pressures and other indirect human impacts. Therefore, our findings support a re-evaluation of this species' conservation status.

Keywords: Eagle Rays, *Aetobatus laticeps*, conservation genetics, Bayesian phylogenetics, population genetics, Eastern Tropical Pacific, Phylogeography.

RESUMEN

La raya águila moteada del Pacífico Oriental Tropical (POT), *Aetobatus laticeps*, es una especie poco estudiada con limitada información sobre su ecología y conservación. Hace solo 10 años, estudios moleculares redescubrieron esta especie como distinta del complejo *Aetobatus narinari* (ANSC). Los estudios que dividieron este complejo no realizaron un muestreo equilibrado, ya que recolectaron 50 individuos en el Atlántico y solamente 5 en el POT. La vasta extensión y heterogeneidad ambiental del POT podrían estar ocultando una proporción significativa de la variación genética del género e incluso nuevas especies. Las rayas águila son especialmente vulnerables a descensos poblacionales debido a su baja fecundidad y alta exposición a pesquerías directas e incidentales. Consecuentemente, cuantificar su diversidad genética, rango de distribución e interconectividad es crucial para evaluar correctamente su estado de conservación. Este estudio utilizó un enfoque de marcadores genéticos mixtos para analizar la filogenia, diversidad genética y filogeografía de las rayas del POT. En primer lugar, se encontró que las rayas águila del POT corresponden a *Aetobatus laticeps*. En Segundo lugar, se detectó niveles alarmantemente bajos de variabilidad genética en todos los marcadores, junto con una fuerte estructuración genética que responde a la geografía. Por último, nuestros datos indicaron tres posibles mecanismos que explican esta estructuración poblacional: A) Aislamiento por distancia, B) Aislamiento por filopatría, y C) Aislamiento por profundidad. El presente trabajo constituye el primer estudio significativo sobre la diversidad genética de las rayas águila en el POT, lo que arroja luz sobre una especie previamente ignorada. Los hallazgos destacan su alta susceptibilidad a las presiones pesqueras y a impactos humanos indirectos. Los autores subrayan la necesidad urgente de reevaluar su estado de conservación.

Palabras clave: Rayas águila, *Aetobatus laticeps*, genética de la conservación, filogenética bayesiana, genética de poblaciones, Pacífico Oriental Tropical, Filogeografía.

TABLE OF CONTENTS

INTRODUCTION	11
METHODOLOGY	14
Sampling	14
DNA extraction	15
Primer design	15
PCR Amplification	16
Sequence Validation and alignment.	17
Haplotype Networks	18
Fixation indexes, Amova and cluster analysis	19
Phylogenetic trees	20
Resistance modelling	21
RESULTS	23
DNA extraction, amplification and sequencing	23
Haplotype networks	23
Heterozygosity, Haplotype and Nucleotide diversity	25
Analysis of Molecular Variance	26
Fixation Indexes	26
Discriminant analysis of principal components (DAPC)	28
Concatenated sequences COI and CYTB	30
Distance vs Resistance isolation modeling	31
DISCUSSION	33
Genetic diversity and connectivity of Eagle Rays in the Eastern Tropical Pacific	33
Population structuring of <i>A. laticeps</i> in the ETP	36
Paleoclimatic fluctuations and current population structuring	38
Species delimitation	39
Relationships with the genus	40
CONCLUSIONS	42
RECOMMENDATIONS	43
Conservation implications	43
Methodological suggestions	43

REFERENCES	45
SUPPLEMENTARY MATERIALS AND INFORMATION	57
Supplementary table 1: List of accessions used for Bayesian Phylogeny outgroups and calibration nodes.....	57
Supplementary figure 1: Bayesia Tree of COI sequences.....	58
COI phylogeny	59
CYTB	59
ITS2	60
Supplementary figure 2. Bayesian Tree of CYTB sequences	61
Supplementary figure 3. Bayesian Tree of Time Calibrated ITS2 Sequences	62
Supplementary figure 4. Bayesian Tree of Time Un-calibrated ITS2 Sequences.....	63

LIST OF TABLES

TABLE 1: ESTIMATES OF HETEROZYGOSITY, NUCLEOTIDE AND HAPLOTYPE DIVERSITY FOR EACH MARKER AND THE COI-CYTB CONCATENATED DATASET.....	25
TABLE 2: RESULTS FROM THE MONTE CARLO TEST OF THE PHI STATISTIC AND THE GENETIC VARIATION COMPONENTS	26
TABLE 3: GLOBAL AND PAIRWISE FIXATION INDEXES.....	27

LIST OF FIGURES

FIGURE 1: STUDY AREA.....	14
FIGURE 2: HAPLOTYPE NETWORK AND HAMMING DISTANCE HEATMAP OF CONCATENATED MITOCHONDRIAL SEQUENCES	24
FIGURE 3: DISCRIMINANT ANALYSIS OF PRINCIPAL COMPONENTS OF CONCATENATED COI AND CYTB SEQUENCES.....	29
FIGURE 4: CALIBRATED BAYESIAN PHYLOGENY OF CONCATENATED CYTB AND COI SEQUENCES	31
FIGURE 5: LEAST COST PATHS MAP: 300-METER DEPTH LIMITATION VS. NO DEPTH LIMITATION. .	32

INTRODUCTION

The Aetobatidae family encompasses one genus, *Aetobatus* (White & Naylor, 2016), which has recently undergone several taxonomic revisions resulting in the emergence, or in some cases, the resurgence of several eagle ray species (Richards et al., 2009c; Sales, de Oliveira, et al., 2019; White et al., 2010). Most of these new species have originated from the taxonomic reclassification of the spotted eagle ray, *Aetobatus narinari* (Euphrasen, 1790).

As is the case with most species exhibiting a cosmopolitan distribution, *A. narinari* was long suspected to be an intricate cryptic species complex. Differences in the parasitic communities of geographically distant *A. narinari* populations led researchers to seriously question the species' pantropical occurrence (Richards et al., 2009c). Only in the last decade with the advent of molecular tools for species delimitation, was the *A. narinari* species complex (ANSC) conclusively partitioned into at least two independently evolving taxa [i.e., species] (*A. narinari* in the Atlantic Ocean, *A. ocellatus* (Kuhl, 1823) in the Indian Ocean and Western Pacific). A third lineage, *A. laticeps* (Gill, 1865) in the Eastern Tropical Pacific is still somewhat debated. The phylogenetic relationships between the three species that once formed the ANSC appear to be the result of two vicariant or dispersal speciation events. The first, estimated to have happened 3.7 million years ago (Mya), isolated the Indo-Pacific (*Aetobatus ocellatus*) eagle rays from those in the Atlantic (*Aetobatus narinari*) and Eastern Pacific (*Aetobatus laticeps*) (Richards et al., 2009c; Sales, de Oliveira, et al., 2019). A second event, estimated at 1.4 Mya, further divided the Atlantic eagle rays from those in the Eastern Pacific (Richards et al., 2009c; Sales, de Oliveira, et al., 2019). Richards et al., (2009c) theorized that the formation of the Panama Isthmus formed a barrier that disconnected gene flow between the Atlantic and the Eastern Pacific populations. However, Sales et al., (2019) questioned this hypothesis because

they found that the isthmus formation event preceded the divergence of the Eastern Pacific and Atlantic lineages of eagle rays by two to four million years, depending on the isthmus formation estimate.

Richards et al., (2009c) and Sales et al., (2019) suggest that the most likely point of origin of the ANSC occurred in the Indo-Pacific and that it later radiated westward towards the Atlantic and finally to the Eastern Pacific. This westward migration was probably facilitated by the east-to-west direction of the oceanic currents generated by trade winds (Denny, 2008). Trade wind currents and Walker cells in the Pacific might also explain why the ANSC did not directly reach the Eastern Pacific from its point of origin in the Indo-Pacific (Denny, 2008). Though currents that flow in the opposite direction (west to east) caused by westerlies do exist, they occur at cold subtropical latitudes, and are therefore probably inaccessible to species adapted to warmer temperatures.

Of the lineages that make up the ANSC, *Aetobatus laticeps*, the Eastern Pacific (EP) lineage, is the least studied on a molecular level. For example, Sales et al., (2019) only used two individuals from the same locality on the Pacific Mexican coast to map the phylogeography of the *Aetobatus* genus, while taking 24 samples at multiple Atlantic localities. Similarly, Richards et al. (2009) only used six samples from two localities in the EP, while using 24 samples from five sites in the Caribbean alone. This underrepresentation of *A. laticeps* in molecular studies has probably obscured the entire genus's genetic diversity and might have also resulted in biased sampling methods. Furthermore, given the immense size and habitat heterogeneity of the EP, sampling from only a few localities might further obscure genetic variation among different sub-populations.

Because eagle rays, like most batoids, have relatively low fecundity, they are highly susceptible to population declines caused by both direct fisheries and bycatch pressure (White et al., 2010). Until recently, *A. narinari* was assessed as a single cosmopolitan species, and thus local, small-scale fisheries were deemed to be less of a threat to the species' overall survival (Richards et al., 2009c). However, now that the species has been partitioned, it is highly likely that each of the ANSC component species is worse off than initially thought (Sales, de Oliveira, et al., 2019; Stevens, 2000).

Consequently, adequately delimiting which ANSC species are present in the EP, elucidating how genetically diverse these species might be, and understanding which factors limit gene flow in the EP are of utmost importance to (a) further our knowledge of the *Aetobatus* genus as a whole and, more importantly, (b) adequately assess this species' conservation status and resilience to human pressure.

METHODOLOGY

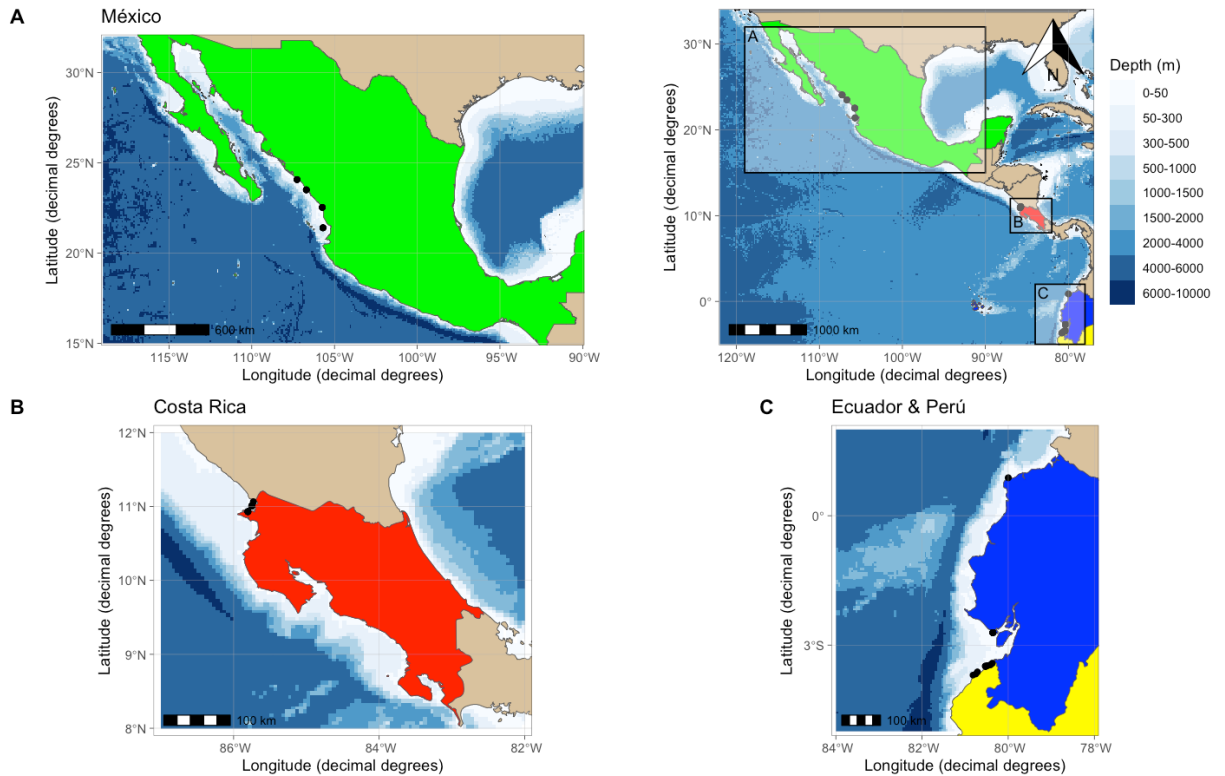


Figure 1: Study Area

This map displays our sampling sites across the Eastern Tropical Pacific Ocean. Sampling was carried out in four countries which are highlighted on panels A, B and C. (A for Mexico, B for Costa Rica and C for Ecuador and Peru). Sampling sites are depicted as black dots. The ocean floor is overlaid with a false color representing bathymetry, ranging from white (0m) to dark blue (<-4000m) made with data from the General Bathymetric Chart of the Oceans (GEBCO) using the built-in bathymetry option from the R package ggOceaMaps.

Sampling

A total of 87 tissue samples were collected from four countries in the Eastern Tropical Pacific: 25 samples from Mexico's Gulf of Baja California, 20 samples from Ecuador, 22 from Peru and 20 from Costa Rica (Figure 1). Sample collection techniques varied among sites. Samples collected in Peru and Ecuador were obtained from fishermen as bycatch collected at multiple localities. Mexican samples were collected by scientific vessels conducting research on

experimental trawling as detailed in (Garcés-García et al., 2020). In contrast, tissue samples collected in Costa Rica were taken from live individuals in the water using a Hawaiian sling. Irrespective of the sampling technique, all tissue samples were preserved in 95% ethyl alcohol and stored at -20 °C.

DNA extraction

DNA extractions were carried out using QIAGEN's DNeasy™ Blood and Tissue® extraction kit (Qiagen, Germantown, MD, USA) following the kit's handbook (QIAGEN, 2020, pp. 31–33). After extraction, samples were quantified using NanoDrop™ 2000 spectrophotometer to assess DNA content and quality indexes (Thermo Fisher Scientific, MA, USA). To check for genomic integrity, 3 µl of each DNA sample was mixed with 3µl of BlueJuice™ loading buffer (10x). The loading buffer-sample mixtures were run on a 1% agarose gel with 1.5% SYBR™ Safe stain at 100v for 30 minutes. To preserve sample stocks, samples with DNA concentrations higher than 200 ng/µl were diluted to 100ng/µl aliquots and then further diluted to 20ng/µl aliquots, which is the concentration needed for PCR amplification. Samples with concentrations between 200ng/µl and 40ng/µl were diluted directly to 20ng/µl aliquots. Samples with DNA stock concentrations lower than 40 ng/µl were not diluted.

Primer design

Primer design followed a mixed marker approach (MMA), incorporating both nuclear and mitochondrial regions in order to adequately infer gene flow in a species that might have male-biased dispersal (Phillips et al., 2021; Richards et al., 2009c). The genetic regions analyzed COI, CYTB and ITS2 were selected due to their use in previous eagle ray population genetics studies

(Richards et al., 2009c; Sales, de Oliveira, et al., 2019). The expected amplicon lengths were 766 bp for the COI region, 596 bp for CYTB region, and 740 bp for the ITS2 region. The COI region was amplified using the CO1_Mylio_F2 (5'-GcTTYATYGTcTGAGCCCA-3') and CO1_Mylio_R2 (5'-AGYGGTTATGTGgTTGGCTTGA-3') degenerated primer pair. The CYTB region was amplified using the ANAR CBF1 (5'-GAGGGGCAACTGTCATCACTAACC-3') and ANAR CRB2 (5'-AGCAATTTGTCCGATGGTGA-3') primer pair. The ITS2 region was amplified using the Bat5.8SmF1 (5'-GCTACGCCTGTCTGAGGGTCGC-3') and the Bat28SR1 (5'-ACAGGCTAGGCCTCGATCAGAAGG-3') primer pair. The primer sequences for the reverse ITS2 and the forward CYTB primers were the same as those used in (Richards et al., 2009c), while all other primer sequences were designed in Primer 3 using Chondrichthyes-wide sequence concatenations obtained from GenBank queries.

PCR Amplification

Amplification of the COI and ITS regions used a total PCR volume of 30 µl, including 3 µl of genomic DNA diluted to 20ng/µl according to NanoDrop quantification, 19.3 µl of water, 3 µl of 10X Buffer, 0.9 µl of 50mM MgCl₂, 0.6 µl of 10 mM dNTPs, 1.5 µl of 10 µM forward and reverse primers, and 0.2 µl of 5 units/µl Taq Platinum. Samples were amplified using a ThermoFisher Scientific MiniAmp™ cycler. The thermocycler's temperature profile was the same for both ITS2 and COI primers, except for the annealing step. Thermal cycling began with an initial denaturation at 94 °C for 5 minutes, followed by 35 cycles of denaturation at 94 °C for 30 seconds, annealing at 61 °C (63 for the ITS2 region) for 30 seconds, and extension at 72 °C for 45 seconds. A final extension was carried out at 72 °C for 5 minutes. For ITS2 samples that

didn't amplify under these conditions, 0.3 μ l of BSA (1 mg/ml) were incorporated to the PCR mix, adjusting the water volume to maintain a total final volume of 30 μ l.

Amplification of the CYTB region used a total PCR volume of 27 μ l, which included 3 μ l of genomic DNA diluted to 20ng/ μ l according to NanoDrop™ quantification, 14.35 μ l of water, 2.7 μ l of 10X Buffer, 0.81 μ l of 50mM MgCl₂, 0.54 μ l of 10 mM dNTPs, 2.7 μ l of 10 μ M for both primers, and 0.2 μ l of 5 units/ μ l of Taq Platinum. Amplification was carried out using a ThermoFisher Scientific MiniAmp™ cycler. The thermocycler's temperature profile started with an initial denaturation at 94 °C for 5 minutes, followed by 35 cycles of denaturation at 94 °C for 15 seconds, annealing at 60 °C for 30 seconds, and extension at 72 °C for 1 minute. A final extension was performed at 72 °C for 7 minutes.

All PCR reactions included a sample-free negative control to check for reagent contamination. Following thermal cycling, samples were run on a 1% agarose gel with 1.5% SYBR™ Safe stain, alongside a 100 bp ladder, at 100v for 30 minutes to check for amplicon size, specificity, and negative control contamination.

Amplicons were sent to Macrogen® (Geumcheon-gu, Seoul, South Korea) for sequencing which was performed by capillary electrophoresis using an ABI 3730xl sequencer. Problematic sequences were purified and re-sequenced by Macrogen® until a consensus sequence could be assembled from forward and reverse reads.

Sequence Validation and alignment.

Electropherograms were trimmed and checked for base-specificity before assembling forward and reverse reads into a consensus sequence using Geneious' De Novo Assemble tool.

Consensus sequences were visually inspected against electropherograms in Geneious® to resolve

ambiguous base calls. Any base calls that could not be visually resolved retained their IUPAC uncertainty codes (e.g., R, S, N, etc.). After base-calling, sequences were aligned using Geneious' ClustalW tool, with one alignment performed per region (CYTB, COI, ITS). The alignments were trimmed to ensure all sequences had the same length within each marker. Sequence alignments were exported in FASTA format for statistical and genealogical analysis. Following individual analysis, the COI and CYTB regions were concatenated into a single FASTA file and analyzed as a single 1155 pb locus. Sequences were concatenated in R using a custom-built function.

Haplotype Networks

Sequence alignments were analyzed using the R packages *pegas*, *adegenet*, *ade4*, *apex*, *mmod*, *poppr*, and *msa* within the R studio environment (Bodenhofer et al., 2015; Jombart, 2008; Kamvar et al., 2014; Paradis, 2010; Posit team, 2023; R Core Team, 2023; Schliep et al., 2020; Winter, 2012). Alignments were imported into R as FASTA files and then converted into a *dna.bin* type object to enhance analysis efficiency and reduce memory usage. Haplotypes were calculated using the *pegas* function `haplotypes()`. Haplotype networks were inferred using hamming distances to express genetic relationships between haplotypes, using the *haplonet* function from *pegas*. Hamming distances were selected because the sequences contained gaps and ambiguous base calls. To better visualize the relationships between haplotypes, a heatmap of Hamming distance dissimilarities was made using the `heatmap2` function from the *gplots* package (Warnes et al., 2022).

Fixation indexes, Amova and cluster analysis

To analyze both pairwise and global fixation indexes, the FASTA alignment file was transformed into a *genind* object using apex package's `multidna2genind()` function. This type of object was selected due to its capability to accommodate various superseding strata assignments. Populations were defined according to the sequence grouping within the concatenated alignment, ensuring that all sequences from each population were grouped together.

Fixation indexes including GST, Φ_{st} , Jost's D, H_s and H_t were calculated using the `diff_stats()` function from the `mmod` package (Winter, 2012). Pairwise fixation indexes calculated included Nei's GST, Hedrick's GST and Jost's D, which were selected because they employ different algorithms and represent distinct concepts. Jost's D calculates differentiation directly, providing a monotonic and accurate representation of subpopulation relatedness, which does not vary with intra-population heterozygosity (Jost, 2008). In contrast, early versions of GST, such as Nei's GST, may fail to indicate differentiation in populations with high heterozygosity. This means that even if populations share no alleles, Nei's GST may suggest no differentiation when H_s is high. On the other hand, Jost's D and Hedrick's G_{st} (a standardized version of GST) correctly indicate differentiation when diversity is high (Jost, 2008).

Additionally, GST fails to reflect differentiation when the number of unique alleles increases in each population (Jost, 2008).

Confidence intervals for global differentiation indexes, such as Nei's G_{st}, Hedrick's G_{st}, and Jost's D, were calculated using the `summarise_bootstrap()` function from the `mmod` package. To determine whether genetic variation was greater between or within populations, the `popper.amova()` function from `popper` was used (Kamvar et al., 2014).

Discriminant analysis of principal components (DAPC) was conducted on the sequence data. DAPC was selected due to its computational efficiency in studying genetic clustering within and between populations, offering a more efficient alternative to Bayesian clustering methods (Jombart et al., 2010). Additionally, DAPC does not necessarily require the input of priors and can identify clusters using the k-means algorithm coupled with model selection to determine the optimal number of clusters (Jombart, 2008; Jombart et al., 2010; Jombart & Ahmed, 2011). The number of principal components (PCs) was determined through a-score optimization, that represent the discrimination power based on the number of retained PCs. As more PCs are included, overfitting becomes a concern, and cluster discrimination power decreases (Jombart et al., 2010). We found that retaining two principal components was sufficient to maintain discriminatory power. Similarly, the number of discriminant functions (axes retained in DAPC) was selected based on their eigenvalues. Since only the first two discriminant functions retained any variation, they were selected. The number of clusters was selected based on Bayesian Information Criterion (BIC) during the model selection step. All four clusters were retained, as including all four resulted in the lowest BIC scores (Jombart et al., 2010).

Phylogenetic trees

Sequence alignments for the COI, CYTB, concatenated COI and CYTB, and ITS regions were imported into BEAST2 to infer Bayesian phylogenetic trees. For the COI and concatenated trees, fragments of whole mitochondrial genome accessions from different *Aetobatus* species were used as outgroups, as our COI primers were locally designed no gene-specific (COI) accessions for the *Aetobatus* genus aligned with our sequences. However, since the primers used for CYTB

were consistent with those used by other researchers, we could incorporate numerous more gene specific accessions from different *Aetobatus* species, resulting in more informative tree analyses.

Marker specific accession lists are registered in supplementary table 1

Tree priors were configured in BEAUTi. The HKY model was chosen as the substitution model, with the proportion of invariants, substitution rate, and kappa parameter set to be estimated by the program. A Yule-calibrated speciation model was selected, considering that all species analyzed, including the outgroup, are currently extant and represent distinctly evolving lineages. Birth rates were modeled with a gamma distribution, with the alpha parameter set to 0.01 and beta to 1000. The divergence between *Aetobatus ocellatus* and the rest of the lineage, previously estimated by Richards et al., (2009) and Sales et al., (2019) at 3.7 million years ago, was used as the calibration node for both the COI and concatenated trees. For the CYTB tree, two calibration nodes were used: the aforementioned *A. ocellatus* divergence and the divergence of the western Pacific *A. flagellum*, estimated at 18.7 million years ago by.

Tree posterior distribution densities were assessed in Tracer. The best-supported tree was selected using TreeAnnotator, with a burn-in percentage of 10%, a posterior probability limit of 0, and the target tree type set to maximum clade credibility. Trees were visualized using the ggtree package in R.

Resistance modelling

To understand the role of the environmental factors contributing to on geographic isolation observed amongst haplotypes, we compared an isolation by distance model and an isolation by resistance model, using depth as the primary explanatory variable. Depth was validated as a significant factor in species distribution using maximum entropy modeling in R, using eagle ray

observations from the Eastern Tropical Pacific available on GBIF using the `dismo` package (Hijmans et al., 2023). Our goal was to determine whether population differentiation was solely due to geographic distance or if environmental features provided a better explanation for the observed genetic diversity patterns. To achieve this, two geographic distance matrices were generated between sampling locations. First, a bathymetric map was obtained using the `getNOAA.bathy()` function from the `marmap` R package (Pante et al., 2023). From this map, two transition probability matrixes were created: one with a 300-depth limit and another with no depth limitation. From each transition matrix we generated a geographic distance matrix between sampling points using a least cost paths algorithm via `marmap`'s `lc.dist()` function (Pante et al., 2023).

RESULTS

DNA extraction, amplification and sequencing

Of the 87 tissue samples collected, we were able to successfully amplify and sequence 72 individuals across all markers. The nuclear marker, ITS2, was the most problematic to both amplify and sequence producing 75 usable sequences with a length of 471 bases of the expected 740. The mitochondrial markers on the other hand, produced an average of 80 usable sequences. The COI sequences had a length of 649 bases of the expected 766, while the CYTB sequences were 506 bases long of the expected 596. We had to reduce the sample set to 72 to have the same sequences across all markers in order to make adequate diversity comparisons between them.

Haplotype networks

We identified nine haplotypes within the concatenated COI and CYTB regions from samples collected in the Eastern Tropical Pacific. In contrast, we found a single ITS2 sequence type amongst all collected samples. Figure 2 shows a clear geographic segregation of the concatenated COI and CYTB haplotypes. For example, many unique haplotypes were identified from the samples taken in Costa Rica and Mexico, while a single haplotype was shared between Ecuador and Peru. The various haplotypes found both in Costa Rica and Mexico were more closely related to other haplotypes found in the same population than those taken at different sites. Figure 2 shows the hamming distances between haplotypes varied from one to seven bases. The most divergent haplotype, H9, represented by a single sequence from Peru, differed from other haplotypes by five to seven bases, with the fewest differences (5) from haplotype H1, composed of samples from Mexico. Additionally, we observed a marked difference in internal diversity among populations. While only two haplotypes were present between the samples from

Peru and Ecuador, Mexico had four haplotypes, and Costa Rica had three. Furthermore, individuals were more evenly distributed among haplotypes in Costa Rica, than in Mexico, Peru and Ecuador.

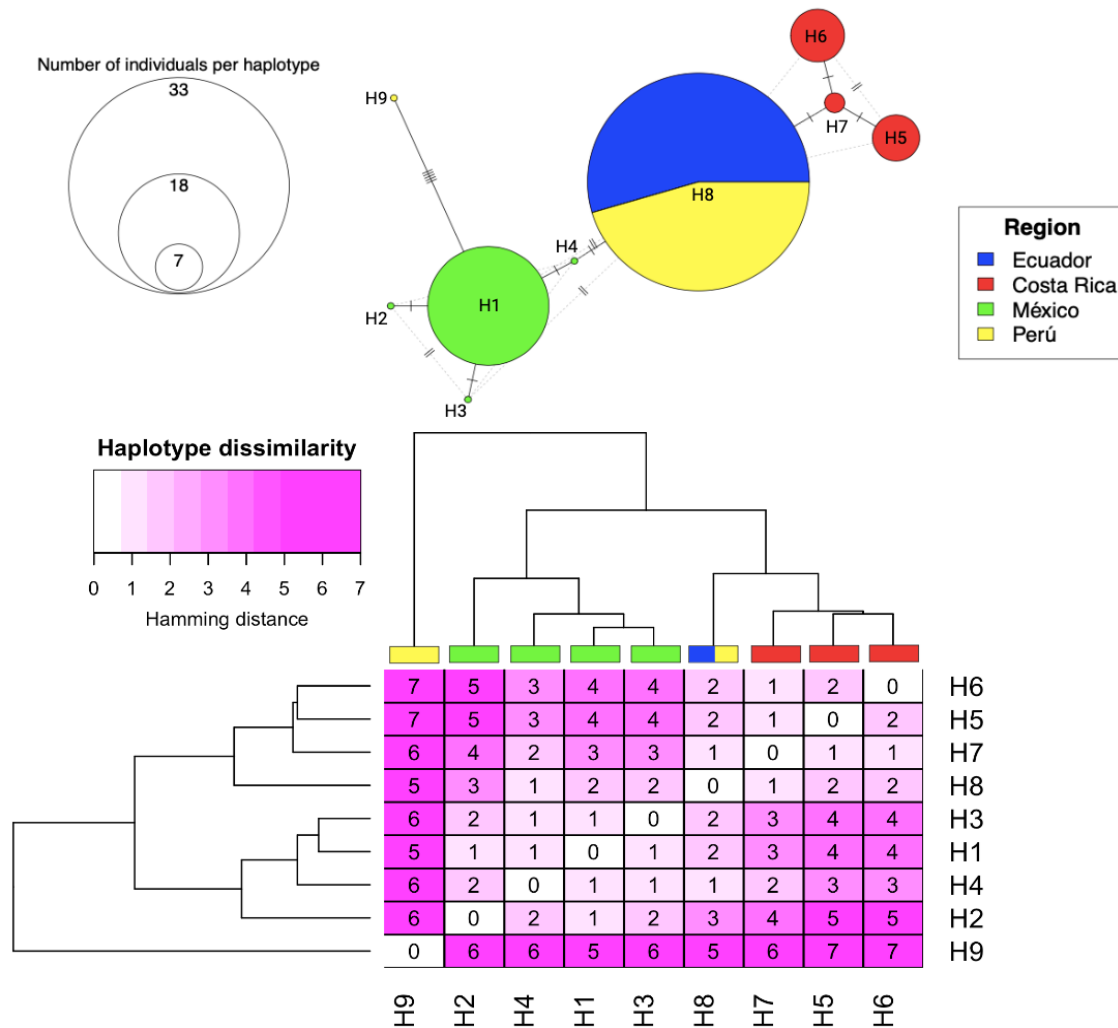


Figure 2: Haplotype Network and Hamming Distance Heatmap of concatenated mitochondrial sequences

Figure 2 depicts Haplotype Networks in panel A and Hamming distance Heatmaps calculated from concatenated COI and CYTB sequences in panel B. In the Haplotype Network in panel A, the diameter of the circles is proportional to the number of individuals that are present in each Haplotype. The colors in the circles represent the countries from which the samples were collected. The Hamming Distances in the Heatmap in panel B are colored according to the number of different bases between each Haplotype. The color scales from white, representing no base differences, to different scales of magenta that darken with the number of base differences between sequences.

Heterozygosity, Haplotype and Nucleotide diversity

Subpopulation heterozygosity for the concatenated mitochondrial markers ($H_s=0.2568909$) was substantially lower than total Heterozygosity ($H_t=0.6970352$). Since H_s was smaller than H_t , global genetic variation exceeded subpopulation genetic variations. This trend can be observed to varying degrees when analyzing both mitochondrial markers individually. CYTB presented a larger difference between total and subpopulation heterozygosity, at 0.1903 and 0.641 respectively. The difference between H_s and H_t was higher still in COI, with H_s at 0.09659, and H_t at 0.6387, implying a difference in the differentiation rates between these two markers. ITS2 followed the same pattern, although to a lower degree, with H_s at 0.2443 and H_t at 0.5185 (Table 1).

When analyzing the concatenated COI-CYTB alignment, we found that, on average, there were approximately $1.013831e-03$ base differences per site between any two sequences, with a variance of $5.353463e-07$ bases. Globally, haplotype diversity (H_d) was notably high, around 72.1 % with a variance of less than 0.5%, indicating a high probability of finding two distinct haplotypes when randomly sampling pairs of sequences. When analyzed separately, both mitochondrial markers had similar levels of nucleotide diversity, but lower levels of haplotype diversity. Conversely, ITS2 presented no haplotypic or nucleotide diversity (Table 1).

Table 1: Estimates of heterozygosity, nucleotide and haplotype diversity for each marker and the COI-CYTB concatenated dataset.

Locus	Subpopulation Heterozygosity (H_s)	Total Heterozygosity (H_t)	Nucleotide Diversity (N_d)	Haplotype Diversity (H_d)
Concatenated mt	0.25689093	0.6970352	1.01E-03	0.72108067
CYTB	0.1904271	0.6400547	5.85E-04	0.651087309
COI	0.09659391	0.6387318	1.28E-02	0.683024691
ITS	0.24428371	0.5185224	0	0

Analysis of Molecular Variance

The analysis of molecular variance (AMOVA) of the concatenated sequences revealed that genetic variation was higher between populations (68.98%) than within populations (31.02%) (Table 2). These differences between populations were statistically significant ($p=0.01$) as demonstrated through Monte Carlo test with 999 permutations. The observed value of the phi statistic was almost five times higher than the expected value under a model that assumes no genetic structuring, as shown in Table 2.

Table 2: Results from the Monte Carlo Test of the Phi statistic and the genetic variation components

Monte Carlo Test			
Expected Value	Observed Value	Simulated p-value	Variance
0.329629e-04	0.5970928	0.01	3.948013e-04
Variation composition			
Variation Component	Sigma	Variation (%)	
Between Populations	0.5970928	68.98161	
Within Populations	0.2684898	31.01839	
Total	0.8655826	100	

In the upper half of table 2 that displays the results from the Monte Carlo Test of AMOVA, the distribution of simulated Phi Statistic values from a null model is compared with the actual observed Phi Statistic, the variance and the p-value from the comparison are displayed to the right. The lower half of Table 2 shows the different variance components; intra and inter population variation, and their standard deviation (sigma).

Fixation Indexes

All fixation indexes, both in global and in pairwise comparisons, were high, in some cases equal to 1. Global fixation indexes ranged from 0.631452 to 0.942614, obtained from GST and PhiST respectively. However, the other two measures, Jost's D and Gprime st, were closer to PhiST than GST, with values of 0.7897348 and 0.935982, respectively. Table 3 presents the results for each locus and for the concatenated sequences. When analyzed separately, both mitochondrial

markers presented higher values for all fixation indexes, with COI sequences showing the highest differentiation. On the other hand, ITS2 sequences had lower differentiation than the mitochondrial markers, both individually and when concatenated. However, except for Jost's D, the fixation indexes were still above 0.5.

Table 3: Global and pairwise fixation indexes.

Global Comparisons				
Locus\Measurement	Gst	Gprime_st	D	Phi_St
Concatenated COI and CYTB	0.631452	0.935982	0.7897348	0.942614
CYTB	0.7024831	0.9374472	0.7405182	0.9464214
COI	0.8487723	0.9764409	0.8001391	0.9773822
ITS	0.528885	0.7932771	0.4838477	0.7616545
Pairwise Concatenated Subpopulation Comparisons				
Pairing\Measurement	Nei's GST	Hedrick's GST	Jost's D	
Ecuador-Costa Rica	0.51442308	1	1	
Ecuador-Mexico	0.76573337	1	1	
Ecuador-Peru	0.01728844	0.03617325	0.03617325	
Costa Rica-Mexico	0.37678869	1	1	
Costa Rica-Peru	0.44761357	1	1	
Mexico-Peru	0.67621665	1	1	

The upper panel of table 3 indicates four fixation indexes calculated on a global level, Gst, Gprime st, Jost's D, and Phi_st for the 3 loci analysed, and the concatenated COI and CYTB sequences. The lower of table 3 panel contains the results from three different pairwise fixation indexes Nei's GST, Hedrick's Pairwise GST and Jost's D, calculated from the concatenated COI and CYTB sequences of each country sampled.

At the pairwise level, gene flow between most subpopulation pairs appeared to be substantially restricted. Only Peru and Ecuador presented very low pairwise fixation indexes (i.e., <0.5) across all measurements. Jost's pairwise D and Hedrick's pairwise GST were equal to one for all pairings except for Ecuador and Peru. On the other hand, Nei's Pairwise GST showed that no two subpopulations were completely differentiated from one another. Interestingly, according to Nei's pairwise GST, the subpopulations from Ecuador and Peru were more closely

related to the subpopulation from Costa Rica than the Mexican subpopulation. Conversely, the Mexican subpopulation was more closely related to the population from Costa Rica than the other two subpopulations.

Discriminant analysis of principal components (DAPC)

DAPC revealed five visually distinguishable clusters among concatenated COI and CYTB sequences. These clusters responded to geographic proximity, with three clusters: one for Costa Rica, one for Mexico, and a common cluster formed by samples from Ecuador and Peru. However, some samples were more genetically similar to individuals collected in different sites. For example, AMX_01, AMX_02, AMX_06 and Pal_17 all clustered with samples from Costa Rica. This result differs from the pattern observed in the Haplotype Network in Figure 2, where all Mexican haplotypes were more similar to each other than with those from Costa Rica. Similarly, in Figure 2, haplotype H9 (which corresponds to individual Pal_17) was more closely related to samples from Mexico than it was to those from Costa Rica. Despite these discrepancies, DAPC confirms that there is a clear genetic structuring that generally conforms with geographic proximity.

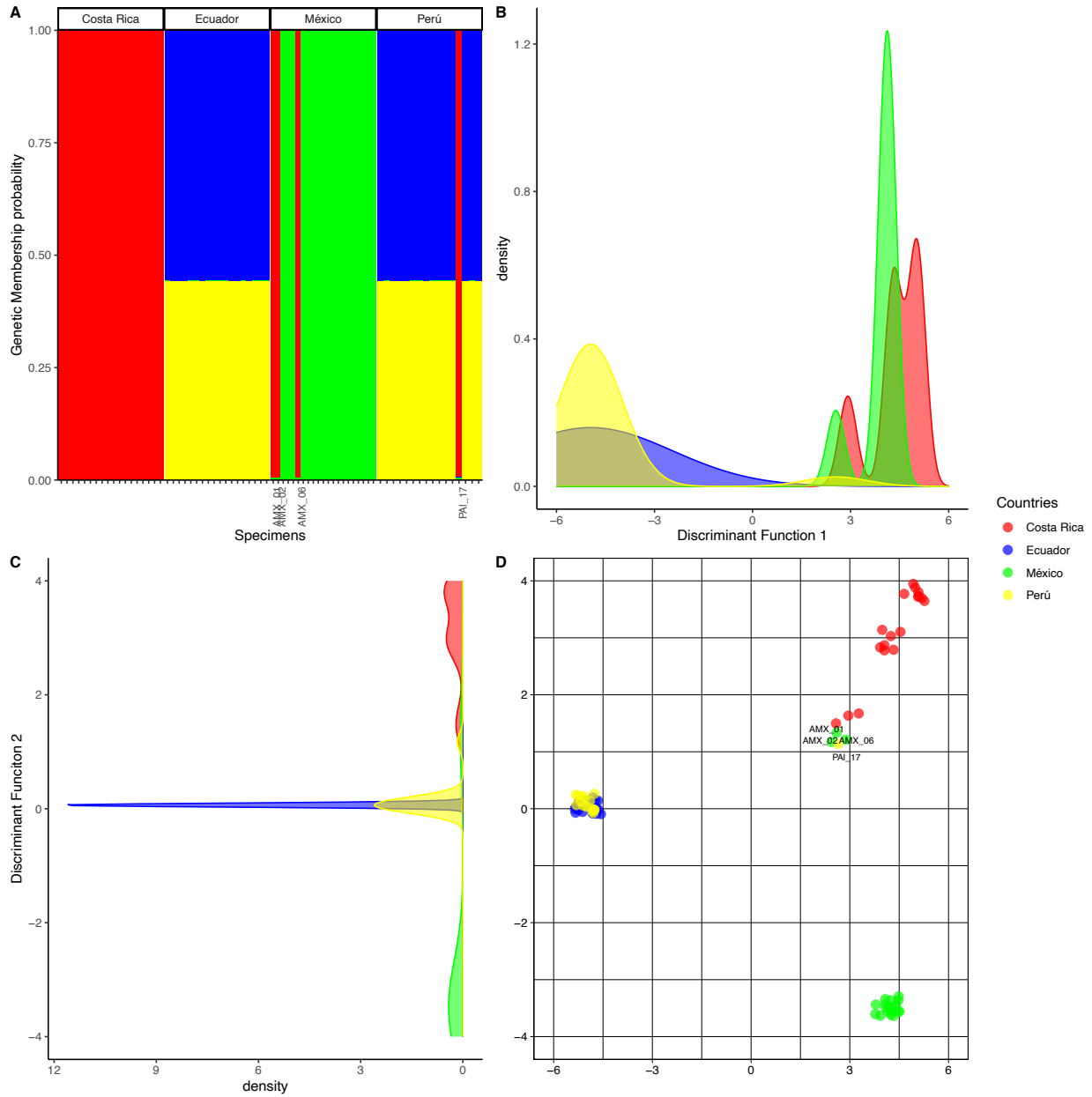


Figure 3: Discriminant Analysis of Principal Components of concatenated COI and CYTB Sequences.

Figure 3 illustrates the genetic clustering of individuals according to Discriminant Analysis of Principal Components DAPC. The figure is divided into 4 different panels: (A), (B), (C), and (D). Panel (A) shows a STRUCTURE type graph that depicts the genetic membership probability of each individual. The vertical bars represent individuals, which are grouped into 4 facets according to where the samples were collected. Each bar is colored vertically according to their genetic membership probability, not the country from which they were sampled. Panels (B), (C), and (D) portray the ordination of individuals according to their genetic resemblance along two discriminant functions, with (B) and (C) each representing the density distribution of individuals along discriminant function 1 and 2 respectively. Panel (D) indicates how individuals cluster

along both discriminant functions. Bidimensional jittering was applied to facilitate the visual assessment of cluster size and composition

Bayesian Phylogenetic Trees

Concatenated sequences COI and CYTB

The Bayesian inference analysis resulted in a tree that shows that all the samples from our study fall into a single well-resolved node (posterior probability ~ 1) which diverged roughly 500 thousand years ago into three geographically isolated nodes. The first containing only individuals from Costa Rica, another exclusively composed of individuals from Mexico, and the third one composed of individuals from both Ecuador and Peru (Figure 4). In most cases, relationships between individuals from the same populations are not well resolved. Interestingly, the aforementioned, atypical sequences (AMX_01, AMX_02, AMX_06, and PAL_17) did not fall into the same node as the samples from Costa Rica.

The divergence time with accession KX151649, an *A. narinari* specimen collected from the Florida Keys, was estimated to be at about 1.5 million years ago, and the divergence between our sequences and *A. ocellatus* sequence JN184054 collected in Japan was estimated to be about 3.5 million years ago.

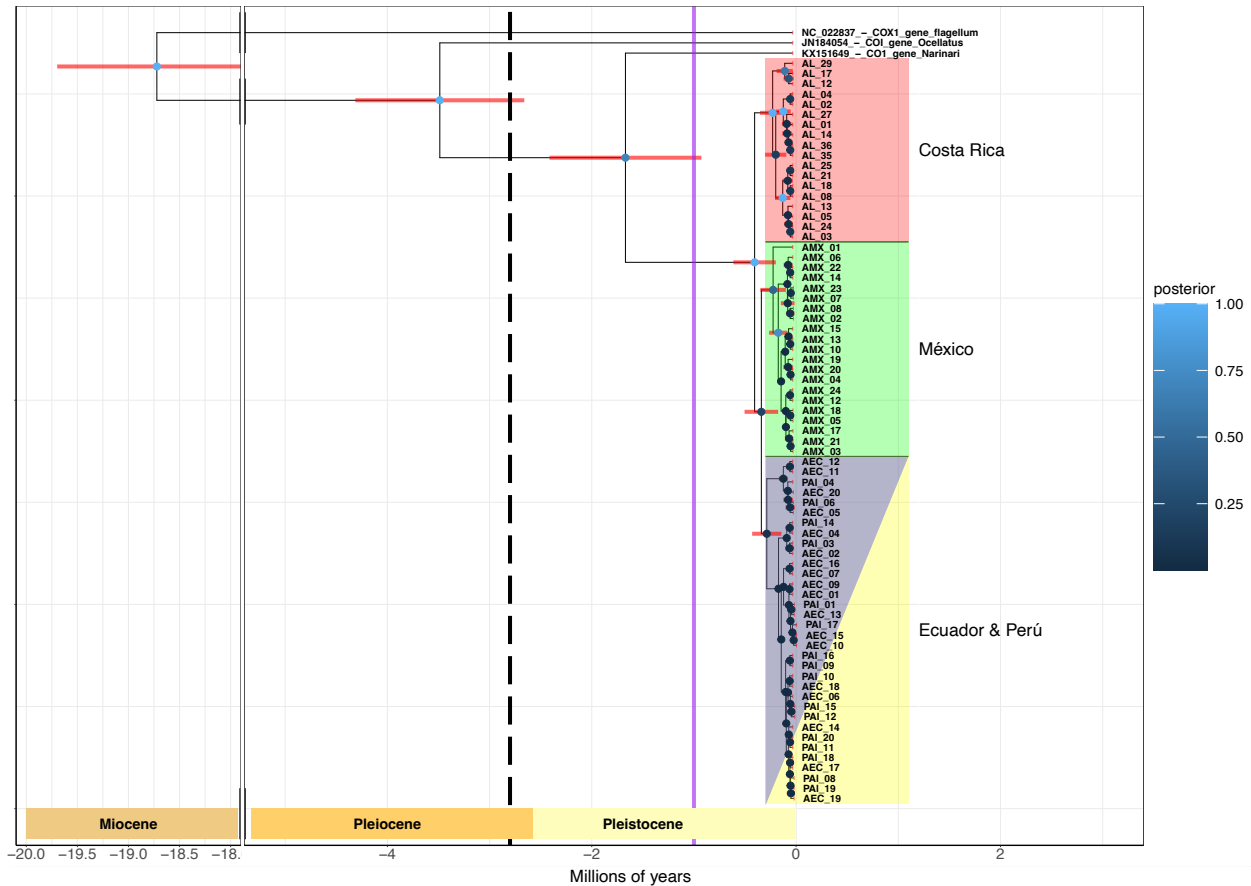


Figure 4: Calibrated Bayesian Phylogeny of Concatenated CYTB and COI sequences

Figure 4 depicts a most recent common ancestor calibrated Bayesian phylogeny of the concatenated COI and CYTB sequences. The dots at each node are colored according to their resolution's posterior probability, lighter tones of blue signify a high posterior probability and a reliable resolution. The red horizontal bars over each node represent the 95% Highest Posterior Density on which each node could land in the temporal scale. The dotted vertical line represents the estimated timing for the formation of the Panamá Isthmus, and the vertical lilac line represents the intensification of the temperature gradient of El Niño Southern Oscillation (ENSO) events. The branches are underlaid with colored boxes indicating the country of origin of each individual.

Distance vs Resistance isolation modeling

We found that the matrix with no depth limitation explained more of the genetic variation and was more significant than the matrix with the depth limitation, $R^2 = 0.0162$, and $p=0.125$, and $R^2=0.17$ and $p=0.00071$ respectively.

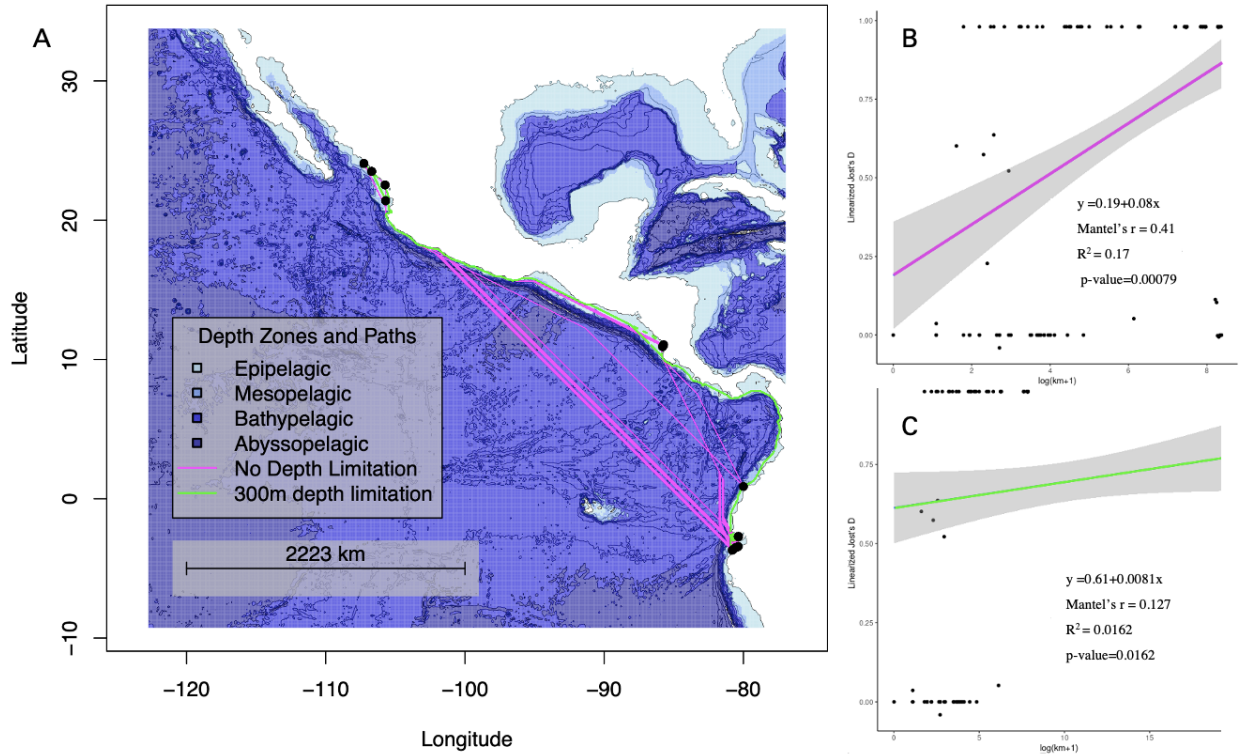


Figure 5: Least Cost Paths Map: 300-meter depth limitation vs. No depth limitation.

Figure 5 is divided into three panels. Panel A represents the study area and is colored according to depth zones. Darker colors represent deeper parts of the ocean. The magenta lines overlaid on the depth zones represent the shortest possible paths individuals could take irrespective of depth. The light green lines that border the coastline represent the shortest possible paths individuals would have to take when a 300-meter depth limitation was inputted into the model. Panels B and C represent the regression between geographic distances between sampling sites and genetic distances between subpopulations under different depth constraints. Geographic distances were log-transformed to make the variation between the vertical axis and the horizontal axis similar in scale.

DISCUSSION

Genetic diversity and connectivity of Eagle Rays in the Eastern Tropical Pacific

This study found a high degree of mitochondrial genetic structuring among eagle ray populations in the Eastern Tropical Pacific. We identified nine novel, geographically segregated haplotypes. Of the nine haplotypes, only one (haplotype H8) was not unique to a single population, as it was shared between Ecuador and Peru. Fixation indexes and Analysis of Molecular Variance (AMOVA) further confirmed significant population structuring that unambiguously responded to geographical separation. Pairwise fixation indexes indicated, in some cases, complete disconnection of gene flow between populations, except for Ecuador and Peru. These results suggest the presence of three genetically isolated populations: one in Mexico, one in Costa Rica, and a single panmictic population shared between Ecuador and Peru. These findings strongly suggest a philopatric tendency and limited dispersal capabilities (Bohonak, 1999; Jaquiéry et al., 2011; Orsini et al., 2013; Prugnolle & de Meeus, 2002).

Subpopulation structuring varied across the four sampling localities. Costa Rica exhibited three evenly represented haplotypes, while Ecuador, Mexico and Peru displayed less internal haplotypic diversity and evenness, each with a single predominant haplotype and smaller, single-individual haplotypes. DAPC ordination reflected a similar pattern: Costa Rica displayed three distinct, evenly sized clusters, whereas Mexico formed one cluster, and Ecuador and Peru formed a single indistinguishable cluster. This structuring could be influenced by sample collection methods. Samples from Ecuador and Peru came from by-catch collected from fishermen, and those from Mexico were collected through deep-water trawling. On the other hand, samples from Costa Rica were collected from live individuals in shallow coastal areas near reefs and mangroves using a Hawaiian sling.

The sampling method employed in Costa Rica might explain why more evenly sized haplotypes were reported in this region as it is likely that it was disproportionately represented by neonates/juveniles and females. A demographic subset that is more prone to evidence genetic structuring in smaller geographic scales due to site fidelity. Acoustic and satellite tagging studies on the Caribbean eagle ray, *A. narinari*, reported both ontogenetic and sex-dependent niche shifts, where females and juveniles were found to spend longer periods of time in coastal areas, where food and protection are more easily accessible (Ajemian & Powers, 2014; Cuevas-Zimbrón et al., 2011; Yokota & Lessa, 2006). Furthermore, the same studies reported multiyear female site-fidelity to coastal ecosystems. Consequently, collecting samples in shallow waters may result in more structured populations compared to deeper water sampling shoals (Ajemian & Powers, 2014; DeGroot et al., 2021).

The DAPC ordination largely aligned with the patterns observed in the haplotype network and fixation indexes. However, it also indicated some level of admixture, as seen in the assignment of four individuals (AMX01, AMX02, AMX06, and PAL17) to one of the clusters from Costa Rica rather than to a cluster with individuals from the same localities (Figure 3, panel D). Therefore, while these results indicate a clear geographic genetic structuring coherent with philopatry, they also indicate a limited degree of individual mobility and population admixture. Differences between DAPC and both Haplotype Networks and Fixation indexes can be attributed to the different approaches these methods use for population assignment. While both Fixation Indexes and Haplotype Networks assign populations on an a-priori basis, DAPC assigns population based on genetic resemblance using several model selection steps and k-means algorithms (Jombart et al., 2010; Miller et al., 2020). Therefore, in this case, the a-priori based methods we applied were incapable of detecting migrants and this limited their ability to

adequately define, genetically homogeneous populations (Meirmans, 2012a, 2015; Miller et al., 2020; Palsbøll et al., 2007).

While the haplotypes were mostly unique to their sampling locality, they exhibited limited divergence, differing by up to seven base substitutions (averaging at 3.1622 base substitutions) in a 1156 bp alignment of concatenated CYTB and COI sequences. A similar trend was observed in high haplotype diversity ($Hd \approx 0.7$) alongside with low nucleotide diversity ($\pi \approx 0.004$), suggesting recent demographic expansion from a smaller ancestral population, because rapid population growth typically results in the appearance of new genetic variants. However, due to the short time scale, the amount of mutations that can arise between these variants is limited (Avice, 2000; Ramos-Onsins & Rozas, 2002; Slatkin, 1987). These findings, coupled with geographic haplotype, suggests that the discontinuance of gene flow between populations is recent, and may hint at founder effects as a mechanism of speciation within *Aetobatus* over short geo-temporal scales (Paulay & Meyer, 2002).

Interestingly, mitochondrial diversity was high, while nuclear variability was minimal, as evidenced by a **single** ITS2 “haplotype”, and lower values in fixation indexes for the ITS marker when compared to mitochondrial markers. Both Richards et al., (2009) and Sales et al., (2019) reported less haplotypes using the ITS2 marker than either the COI or CYTB markers, with Richards et al., (2009c) only reporting seven different ITS2 haplotypes from samples taken from three different species coming from the Eastern Pacific, Western Pacific, and central Atlantic oceans combined and 25 haplotypes from the CYTB marker alone (Richards et al., 2009c). This might be explained by differing mutation rates between the two mitochondrial **coding** sequences we used (COI and CYTB) and the nuclear **non-coding** ITS2, with mitochondrial markers mutating about 20 times faster on average in vertebrates (Allio et al., 2017). This discrepancy

could reflect male-biased dispersal patterns, as mitochondrial genes are maternally inherited, and male-biased movement could lead to faster differentiation in mitochondrial markers than biparentally inherited markers, (Prugnolle & de Meeus, 2002). Male-biased dispersal would be coherent with both the reproductive and the foraging behavior of Eagle Rays, and is also consistent with other ovoviviparous elasmobranchs (Ajemian & Powers, 2014; Phillips et al., 2021; Roycroft et al., 2019). Nevertheless, the addition of more nuclear markers is required to better understand population structure and gene flow patterns in the region (Fuentes-Pardo & Ruzzante, 2017; Hirschfeld et al., 2021; Kowalczyk et al., 2021).

Overall, our findings reveal genetic structuring among *A. laticeps* populations in the Eastern Tropical Pacific, similar to, or greater than that of the genus' other species in the Atlantic and Caribbean, *A. narinari*, and Central and Western Pacific species, *A. ocellatus* (Richards et al., 2009c; Sales, de Oliveira, et al., 2019).

Population structuring of *A. laticeps* in the ETP

Barriers to dispersal are relatively well understood for elasmobranchs. Hirschfeld et al. (2021) found that depth related geographical features explained most of the genetic population structuring patterns across species with different habitat preferences. Importantly, they found that bathymetric features interact in different ways and in different scales depending on a species' habitat preferences. For example, benthopelagic species were found to differentiate due to discontinuances of suitable shallow habitats, while deep demersal species showed limitations to gene flow in the presence of shallow straits separating ocean basins, like the Gibraltar strait. *Aetobatus laticeps*, as other species from the genus, displays benthic habitat preferences (Ajemian & Powers, 2014; DeGroot et al., 2021). Therefore, we hypothesized that bathymetry

might further strain gene flow between populations by forcing individuals to take more indirect routes that skirt the shoreline to get from one location to another.

When comparing the depth limited (longer dispersal paths alongside the coastline) vs the no-depth limitation (shorter pelagic paths) scenarios, we found that the latter explains more and much more significantly the genetic variation between sampling sites ($R^2= 0.0162$, $p=0.125$ and $R^2=0.17$ and $p=0.00071$ respectively) (Figure 5 panels A, B, and C). Depth is unquestionably a barrier for eagle rays due to their habitat preferences, and our results are congruent with its role in the population differentiation of *A. laticeps*. However, its influence at smaller geographical scales without suitable habitat discontinuances is less clear. The correlation coefficients found in this study are low, and we acknowledge the need for further analysis (e.g. testing multiple hypothesis against each other, using causal modelling, or partial mantel tests, instead of direct mantel tests, (Cushman & Landguth, 2010) to reach a more definitive conclusion, considering that inferences from mantel tests tend to be spurious, even when the correlation coefficients are high (Cushman & Landguth, 2010). Similarly, differences in significance levels between tests might be masking spatial autocorrelation of genetic diversity that is not considered under the island model that underlays the mantel test (Hardy & Vekemans, 1999; Meirmans, 2012b; Sokal & Wartenberg, 1983).

Furthermore, as we discussed before, the population structuring we evidenced is could be consistent with female philopatry, a behavior induced obstruction to gene flow, that has been known to obscure the influence that environmental dispersal barriers might have on population structuring (Hirschfeld et al., 2021).-To better understand the role bathymetry, and for that matter any other landscape environmental features might play in this species' population structuring

requires more controlled sampling collection techniques, where sampling continuity, population pairing that controls for distance, and equal sample sizes are considered (Hirschfeld et al., 2021).

Paleoclimatic fluctuations and current population structuring

Bayesian phylogeny of the concatenated mitochondrial markers revealed that there was a ~500,000-year divergence between the three genetic populations we observed in the haplotype network lending credence to our inference of recent divergence due to limited haplotype differentiation. We have already discussed several mechanisms that may account for the genetic structuring observed, including behavior-driven isolation due to philopatry, isolation by distance, and isolation by environmental resistance, specifically depth. However, there is another factor worth considering: paleoclimatic variation.

Over the last ten million years, climatic conditions in the Eastern Tropical Pacific have been highly unstable, with repeated significant sea level changes driven by glacial cycles (Dyez et al., 2016; Fedorov et al., 2006; Lawrence et al., 2006; Medina-Elizalde & Lea, 2005). During this period, surface ocean temperatures have also experienced drastic shifts, alternating through warming cycles (Dyez et al., 2016). Short-term oceanic variability fluctuated significantly, as evidenced by changes in both the period and amplitude of El Niño Southern Oscillation (ENSO) temperature patterns (Fedorov et al., 2006). Oceanic current systems underwent substantial shifts, with the Walker cell re-emerging only around three million years ago (McClymont & Rosell-Melé, 2005).

These factors could reasonably account for the observed genetic structuring between populations. For instance, the shift from a stable El Niño-like state to a cooler, oscillatory state around three million years ago might have fragmented a previously connected, large, panmictic

population into smaller, isolated groups due to thermal constraints on eagle ray activity and reduced habitat availability. Additionally, the increased temperature variation between ENSO phases roughly 1 million years could have led to population declines, as intense changes between ENSO phases have been linked to elevated mortality in several Eastern Tropical Pacific species (Bustamante et al., 2000; Lamb et al., 2018; Laurie, 1990; Salazar P & Bustamante, 2003; Steinfartz et al., 2007; Trillmich & Limberger, 1985; Valle et al., 1987). Similarly, glaciation-driven sea level reductions might have drastically reduced suitable eagle ray feeding and breeding habitats, possibly causing significant mortality events (Ludt & Rocha, 2015).

However, these are mere speculations, to rigorously test how paleoclimatic shifts impacted eagle ray population dynamics during the mid-Pleistocene, more targeted analyses are necessary. For example, demographic reconstructions using Bayesian skyline plots in conjunction with generalized linear models (GLMS) could help evaluate the influence of different paleoclimatic shifts on ancient populations of eagle rays (Grandi et al., 2018; Hirschfeld et al., 2021; Leuenberger & Wegmann, 2010; Nater et al., 2015; Oliveira et al., 2017).

Species delimitation

Bayesian phylogeny of the CYTB marker (Supplementary figure 2) showed that our sequences closely branched with accession MK340528, one of the type-specimens used by Sales et al., (2019) to re-describe *A. laticeps* as a distinct species. Supporting the notion that *A. laticeps* is a distinct species that is native to the Eastern Tropical Pacific (Richards et al., 2009c; Sales, de Oliveira, et al., 2019; White et al., 2010; White & Naylor, 2016). Importantly, BLAST queries could not be trusted for species identification both because most if not all NCBI accessions from

the eastern tropical pacific eagle rays are still cataloged as *A. narinari* and because most accessions are not geo-localized.

Relationships with the genus

The concatenated COI-CYTB phylogenetic analysis indicated that our samples from the Eastern Tropical Pacific form a distinct and well-defined clade that separated from their Atlantic and Caribbean relatives approximately 1.8 million years ago. This clade further split into three different branches around 500,000 years ago, each displaying a geographically segregated pattern consistent with the structuring observed in the haplotype network. This suggests a clear historical divergence between populations within the Eastern Tropical Pacific region.

The divergence between eagle ray populations in the Caribbean and Eastern Tropical Pacific appears to have occurred well after the final formation of the Panama Isthmus, estimated by O’Dea et al., (2016) to have completed 2.8 million years ago, roughly 1 million years before the split between the Caribbean *A. narinari* and our samples. However, the 95% HPD range of this divergence spans over 1 million years, meaning that the split could potentially have occurred up to 0.5 million years earlier. These findings align with Sales et al., (2019), who also observed that the separation between Eastern Pacific and Caribbean lineages postdated the Panama Isthmus’ closure.

These results support growing evidence suggesting that the permeability of the Panama Isthmus to gene flow has fluctuated over time, likely influenced by global climatic events, such as eustatic sea level changes and interglacial periods (Avila-Cervantes et al., 2021; Erkens & Hoorn, 2016; Hirschfeld et al., 2021; Marek, 2015; Musher et al., 2020; Ngeve et al., 2016; Silliman et al., 2022). Nonetheless, there is consensus in that the timing of the biological

disconnection of marine species between the Caribbean and the Pacific does not align exactly with the geological formation of the isthmus (Erkens & Hoorn, 2016). These findings highlight the need for more comprehensive genetic studies with a broader genomic data on related species from both sides of the Panama Isthmus to develop a clearer, more accurate timeline for the seaway's closure.

CONCLUSIONS

1. Our results clearly indicate that eagle rays in the Eastern Tropical Pacific correspond to *Aetobatus laticeps*. In the absence of more representative genomic coverage, we are, for now, unable to detect the presence of more species in this region.
2. The eagle ray subpopulations we sampled presented alarmingly low levels of genetic diversity in the markers we evaluated. Nuclear and mitochondrial markers presented vastly different variation patterns, with the nuclear marker (ITS2) exhibiting no genetic variability whatsoever, while mitochondrial markers (COI and CYTB) presented some genetic variability while simultaneously showing a high degree of geographic-genetic structuring.
3. Our data pointed to three possible mechanisms that could explain the population structuring we encountered: A) Isolation by distance suggested by the spatial autocorrelation of genetic distances, B) Isolation by philopatry implied by the difference in genetic variability between nuclear and mitochondrial markers, and supported by tagging studies conducted in species of the same genus, and C) Isolation by resistance hinted at by this species' diet and habitat preferences, and evidenced by the higher correlation coefficient and lower significance level of the no-depth limitation mantel test.

To this date, this is the first and only study to meaningfully assess eagle ray's genetic diversity in the Eastern Tropical Pacific, shedding a small amount of light into a species that has been understudied and ignored for far too long. Pointing to this species increased susceptibility to both direct and by-catch fishing pressures and other indirect human impacts like habitat reduction and climate change. Therefore, our findings support a re-evaluation of this species' conservation status.

RECOMMENDATIONS

Conservation implications

The low genetic variability and the limited amount of gene-flow between populations we evidenced, in conjunction with eagle ray's slow replenishment rates makes the Eastern Tropical Pacific Species *A. laticeps* even more susceptible to human impacts because at the same time as populations become smaller, they become less resilient to change. Therefore, we suggest that Eastern Tropical Pacific Eagle Rays' conservation status should be assessed far more conservatively. To this end, we recommend the following actions:

- 1) Re-classify this species as endangered in all or most of its native range, as it's exposed to the same pressures as it's Atlantic and Caribbean counterparts
- 2) Include this species in the CITES treaties because, like many elasmobranch species in this region, the main driving force behind targeted fisheries may be international markets and not local consumption.
- 3) Prioritize site-based conservation efforts for this species in its preferred coastal habitats.

Methodological suggestions

Genetic structuring conclusions from relatively small genomic subsets should be considered with caution as they only give us a very small glimpse into genetic differentiation patterns. The inclusion of multiple polymorphic nuclear markers would provide a better insight into actual population differentiation, as they would provide a clearer signal, that is not skewed due to differing mutation rates and could clarify our hypothesis about female philopatry (Hirschfeld et al., 2021).

Similarly, whole mitogenome analysis should also be conducted to more robustly verify the conclusions we reached. The addition of more markers proved decisive in our study, as individual mitochondrial markers presented differing phylogenetic resolutions, that in some cases contradicted known evolutionary relationships. Only when analyzing the concatenated markers, did the phylogenetic relationships clarify. Who's to say what could change when whole mitogenomes from multiple individuals are contrasted.

Finally, to test the isolation hypothesis we postulated and to corroborate the genetic structuring conclusions we reached in this opportunistic exploratory study further research is needed. To this end, future studies should collect samples in accordance with a robust experimental design that prioritizes sampling continuity and interspersed (Hirschfeld et al., 2021).

REFERENCES

- Ajemian, M. J., & Powers, S. P. (2014). Towed-float satellite telemetry tracks large-scale movement and habitat connectivity of myliobatid stingrays. *Environmental Biology of Fishes*, 97(9), 1067–1081. <https://doi.org/10.1007/s10641-014-0296-x>
- Allio, R., Donega, S., Galtier, N., & Nabholz, B. (2017). Large Variation in the Ratio of Mitochondrial to Nuclear Mutation Rate across Animals: Implications for Genetic Diversity and the Use of Mitochondrial DNA as a Molecular Marker. *Molecular Biology and Evolution*, 34(11), 2762–2772. <https://doi.org/10.1093/molbev/msx197>
- Aschliman, N. C., Nishida, M., Inoue, J. G., Rosana, K. M., & Naylor, G. J. P. (2012). *JN184054 Aetobatus ocellatus mitochondrion, partial genome* (343169700; Partial Genome JN184054). NCBI Nucleotide Database. <http://www.ncbi.nlm.nih.gov/nuccore/JN184054.1>
- Avila-Cervantes, J., Arias, C., Venegas-Anaya, M., Vargas, M., Larsson, H. C., & McMillan, W. O. (2021). Effect of the Central American Isthmus on gene flow and divergence of the American crocodile (*Crocodylus acutus*). *Evolution*, 75(2), 245–259.
- Avice, J. C. (2000). *Phylogeography: The History and Formation of Species* (Vol. 447). Harvard University Press. [https://books.google.com/books?hl=es&lr=&id=1A7YWH4M8FUC&oi=fnd&pg=PA1&dq=Avice+JC+\(2000\)+Phylogeography:+the+history+and+formation+of+species.+Cambridge:+Harvard+University+Press.+447+p.&ots=LzsI-8iOaN&sig=hvtVFxjaPhWNHF7EcWYunY7dtn8](https://books.google.com/books?hl=es&lr=&id=1A7YWH4M8FUC&oi=fnd&pg=PA1&dq=Avice+JC+(2000)+Phylogeography:+the+history+and+formation+of+species.+Cambridge:+Harvard+University+Press.+447+p.&ots=LzsI-8iOaN&sig=hvtVFxjaPhWNHF7EcWYunY7dtn8)

- Bodenhofer, U., Bonatesta, E., Horejs-Kainrath, C., & Hochreiter, S. (2015). msa: An R package for multiple sequence alignment. *Bioinformatics*, *31*(24), 3997–3999.
<https://doi.org/10.1093/bioinformatics/btv494>
- Bohonak, A. J. (1999). Dispersal, Gene Flow, and Population Structure. *The Quarterly Review of Biology*, *74*(1), 21–45. <https://doi.org/10.1086/392950>
- Bustamante, R., Collins, K. J., & Bensted-Smith, R. (2000). Biodiversity conservation in the Galapagos marine reserve. *Bulletin de l'Institut Royal Des Sciences Naturelles de Belgique*, *70*, 31–38.
- Cuevas-Zimbrón, E., Pérez-Jiménez, J. C., & Méndez-Loeza, I. (2011). Spatial and seasonal variation in a target fishery for spotted eagle ray *Aetobatus narinari* in the southern Gulf of Mexico. *Fisheries Science*, *77*, 723–730.
- Cushman, S. A., & Landguth, E. L. (2010). Spurious correlations and inference in landscape genetics. *Molecular Ecology*, *19*(17), 3592–3602. <https://doi.org/10.1111/j.1365-294X.2010.04656.x>
- DeGroot, B. C., Bassos-Hull, K., Wilkinson, K. A., Lowerre-Barbieri, S., Poulakis, G. R., & Ajemian, M. J. (2021). Variable migration patterns of whitespotted eagle rays *Aetobatus narinari* along Florida's coastlines. *Marine Biology*, *168*(2), 18.
<https://doi.org/10.1007/s00227-021-03821-2>
- Denny, M. (2008). *How the ocean works: An introduction to oceanography*. Princeton University Press.
- Dyez, K. A., Ravelo, A. C., & Mix, A. C. (2016). Evaluating drivers of Pleistocene eastern tropical Pacific sea surface temperature. *Paleoceanography*, *31*(8), 1054–1069.
<https://doi.org/10.1002/2015PA002873>

- Erkens, R., & Hoorn, C. (2016). The Panama Isthmus, “old”, “young” or both? A reply to O’Dea et al. 2016. *Scientific Advances*.
- Fedorov, A. V., Dekens, P. S., McCarthy, M., Ravelo, A. C., deMenocal, P. B., Barreiro, M., Pacanowski, R. C., & Philander, S. G. (2006). The Pliocene Paradox (Mechanisms for a Permanent El Niño). *Science*, *312*(5779), 1485–1489.
<https://doi.org/10.1126/science.1122666>
- Fuentes-Pardo, A. P., & Ruzzante, D. E. (2017). Whole-genome sequencing approaches for conservation biology: Advantages, limitations and practical recommendations. *Molecular Ecology*, *26*(20), 5369–5406. <https://doi.org/10.1111/mec.14264>
- Garcés-García, K. C., Tovar-Ávila, J., Vargas-Trejo, B., Chávez-Arrenquín, D. A., Walker, T. I., & Day, R. W. (2020). Elasmobranch bycatch by prawn trawls in the Gulf of California: First comprehensive analysis and the effect of fish escape devices. *Fisheries Research*, *230*, 105639. <https://doi.org/10.1016/j.fishres.2020.105639>
- Grandi, M. F., de Castro, R. L., Terán, E., Santos, M. R., Bailliet, G., & Crespo, E. A. (2018). Is recolonization pattern related to female philopatry? An insight into a colonially breeding mammal. *Mammalian Biology*, *89*, 21–29.
- Hardy, O. J., & Vekemans, X. (1999). Isolation by distance in a continuous population: Reconciliation between spatial autocorrelation analysis and population genetics models. *Heredity*, *83*(2), 145–154.
- Hijmans, R. J., Phillips, S., Leathwick, J., & Elith, J. (2023). *dismo: Species Distribution Modeling* [Computer software]. <https://CRAN.R-project.org/package=dismo>
- Hirschfeld, M., Dudgeon, C., Sheaves, M., & Barnett, A. (2021). Barriers in a sea of elasmobranchs: From *fishing* for populations to testing hypotheses in population genetics.

Global Ecology and Biogeography, 30(11), 2147–2163.

<https://doi.org/10.1111/geb.13379>

Jaquiéry, J., Broquet, T., Hirzel, A. H., Yearsley, J., & Perrin, N. (2011). Inferring landscape effects on dispersal from genetic distances: How far can we go?: INFERRING LANDSCAPE EFFECTS ON DISPERSAL. *Molecular Ecology*, 20(4), 692–705.
<https://doi.org/10.1111/j.1365-294X.2010.04966.x>

Jombart, T. (2008). adegenet: A R package for the multivariate analysis of genetic markers. *Bioinformatics*, 24(11), 1403–1405. <https://doi.org/10.1093/bioinformatics/btn129>

Jombart, T., & Ahmed, I. (2011). Adegnet 1.3-1new tools for the analysis of genome-wide SNP data. *Bioinformatics*, 27(21), 3070–3071. <https://doi.org/10.1093/bioinformatics/btr521>

Jombart, T., Devillard, S., & Balloux, F. (2010). Discriminant analysis of principal components: A new method for the analysis of genetically structured populations. *BMC Genetics*, 11(1), 94. <https://doi.org/10.1186/1471-2156-11-94>

Jost, L. (2008). G_{ST} and its relatives do not measure differentiation. *Molecular Ecology*, 17(18), 4015–4026. <https://doi.org/10.1111/j.1365-294X.2008.03887.x>

Kamvar, Z. N., Tabima, J. F., & Grünwald, N. J. (2014). Poppr: An R package for genetic analysis of populations with clonal, partially clonal, and/or sexual reproduction. *PeerJ*, 2, e281. <https://doi.org/10.7717/peerj.281>

Kowalczyk, M., Staniszewski, A., Kamińska, K., Domaradzki, P., & Horecka, B. (2021). Advantages, Possibilities, and Limitations of Mitochondrial DNA Analysis in Molecular Identification. *Folia Biologica*, 69(3), 101–111. https://doi.org/10.3409/fb_69-3.12

Lamb, R. W., Smith, F., Aued, A. W., Salinas-de-León, P., Suarez, J., Gomez-Chiarri, M., Smolowitz, R., Giray, C., & Witman, J. D. (2018). El Niño drives a widespread ulcerative

- skin disease outbreak in Galapagos marine fishes. *Scientific Reports*, 8(1), 16602.
<https://doi.org/10.1038/s41598-018-34929-z>
- Laurie, W. A. (1990). Effects of the 1982-83 El Niño-Southern Oscillation event on marine iguana (*Amblyrhynchus cristatus* Bell, 1825) populations on Galápagos. In *Elsevier oceanography series* (Vol. 52, pp. 361–380). Elsevier.
<https://www.sciencedirect.com/science/article/pii/S0422989408700412>
- Lawrence, K. T., Liu, Z., & Herbert, T. D. (2006). Evolution of the Eastern Tropical Pacific Through Plio-Pleistocene Glaciation. *Science*, 312(5770), 79–83.
<https://doi.org/10.1126/science.1120395>
- Leuenberger, C., & Wegmann, D. (2010). Bayesian Computation and Model Selection Without Likelihoods. *Genetics*, 184(1), 243–252. <https://doi.org/10.1534/genetics.109.109058>
- Ludt, W. B., & Rocha, L. A. (2015). Shifting seas: The impacts of Pleistocene sea-level fluctuations on the evolution of tropical marine taxa. *Journal of Biogeography*, 42(1), 25–38. <https://doi.org/10.1111/jbi.12416>
- Marek, C. (2015). *The emergence of the Isthmus of Panama: A biological perspective*.
<https://core.ac.uk/download/pdf/56346438.pdf>
- McClymont, E. L., & Rosell-Melé, A. (2005). Links between the onset of modern Walker circulation and the mid-Pleistocene climate transition. *Geology*, 33(5), 389–392.
- Medina-Elizalde, M., & Lea, D. W. (2005). The Mid-Pleistocene Transition in the Tropical Pacific. *Science*, 310(5750), 1009–1012. <https://doi.org/10.1126/science.1115933>
- Meirmans, P. G. (2012a). AMOVA-Based Clustering of Population Genetic Data. *Journal of Heredity*, 103(5), 744–750. <https://doi.org/10.1093/jhered/ess047>

- Meirmans, P. G. (2012b). The trouble with isolation by distance. *Molecular Ecology*, *21*(12), 2839–2846. <https://doi.org/10.1111/j.1365-294X.2012.05578.x>
- Meirmans, P. G. (2015). Seven common mistakes in population genetics and how to avoid them. *Molecular Ecology*, *24*(13), 3223–3231. <https://doi.org/10.1111/mec.13243>
- Miller, J. M., Cullingham, C. I., & Peery, R. M. (2020). The influence of a priori grouping on inference of genetic clusters: Simulation study and literature review of the DAPC method. *Heredity*, *125*(5), 269–280.
- Musher, L. J., Galante, P. J., Thom, G., Huntley, J. W., & Blair, M. E. (2020). Shifting ecosystem connectivity during the Pleistocene drove diversification and gene-flow in a species complex of Neotropical birds (Tityridae: Pachyramphus). *Journal of Biogeography*, *47*(8), 1714–1726. <https://doi.org/10.1111/jbi.13862>
- Nater, A., Greminger, M. P., Arora, N., van Schaik, C. P., Goossens, B., Singleton, I., Verschoor, E. J., Warren, K. S., & Krützen, M. (2015). Reconstructing the demographic history of orang-utans using Approximate Bayesian Computation. *Molecular Ecology*, *24*(2), 310–327. <https://doi.org/10.1111/mec.13027>
- Ngeve, M. N., Stocken, T. V. der, Menemenlis, D., Koedam, N., & Triest, L. (2016). Contrasting Effects of Historical Sea Level Rise and Contemporary Ocean Currents on Regional Gene Flow of *Rhizophora racemosa* in Eastern Atlantic Mangroves. *PLOS ONE*, *11*(3), e0150950. <https://doi.org/10.1371/journal.pone.0150950>
- O’Dea, A., Lessios, H. A., Coates, A. G., Eytan, R. I., Restrepo-Moreno, S. A., Cione, A. L., Collins, L. S., De Queiroz, A., Farris, D. W., Norris, R. D., Stallard, R. F., Woodburne, M. O., Aguilera, O., Aubry, M.-P., Berggren, W. A., Budd, A. F., Cozzuol, M. A.,

- Coppard, S. E., Duque-Caro, H., ... Jackson, J. B. C. (2016). Formation of the Isthmus of Panama. *Science Advances*, 2(8), e1600883. <https://doi.org/10.1126/sciadv.1600883>
- Oliveira, L. R. D., Gehara, M. C. M., Fraga, L. D., Lopes, F., Túnez, J. I., Cassini, M. H., Majluf, P., Cárdenas-Alayza, S., Pavés, H. J., Crespo, E. A., García, N., Loizaga De Castro, R., Hoelzel, A. R., Sepúlveda, M., Olavarria, C., Valiati, V. H., Quiñones, R., Pérez-Alvarez, M. J., Ott, P. H., & Bonatto, S. L. (2017). Ancient female philopatry, asymmetric male gene flow, and synchronous population expansion support the influence of climatic oscillations on the evolution of South American sea lion (*Otaria flavescens*). *PLOS ONE*, 12(6), e0179442. <https://doi.org/10.1371/journal.pone.0179442>
- Orsini, L., Vanoverbeke, J., Swillen, I., Mergeay, J., & De Meester, L. (2013). Drivers of population genetic differentiation in the wild: Isolation by dispersal limitation, isolation by adaptation and isolation by colonization. *Molecular Ecology*, 22(24), 5983–5999. <https://doi.org/10.1111/mec.12561>
- Palsbøll, P. J., Bérubé, M., & Allendorf, F. W. (2007). Identification of management units using population genetic data. *Trends in Ecology & Evolution*, 22(1), 11–16. <https://doi.org/10.1016/j.tree.2006.09.003>
- Pante, E., Simon-Bouhet, B., & Irisson, J.-O. (2023). *marmap: Import, Plot and Analyze Bathymetric and Topographic Data* [Computer software]. <https://CRAN.R-project.org/package=marmap>
- Paradis, E. (2010). pegas: An R package for population genetics with an integrated–modular approach. *Bioinformatics*, 26, 419–420.

- Paulay, G., & Meyer, C. (2002). Diversification in the tropical Pacific: Comparisons between marine and terrestrial systems and the importance of founder speciation. *Integrative and Comparative Biology*, 42(5), 922–934.
- Phillips, N. M., Devloo-Delva, F., McCall, C., & Daly-Engel, T. S. (2021). Reviewing the genetic evidence for sex-biased dispersal in elasmobranchs. *Reviews in Fish Biology and Fisheries*, 31(4), 821–841. <https://doi.org/10.1007/s11160-021-09673-9>
- Posit team. (2023). *RStudio: Integrated Development Environment for R*. Posit Software, PBC. <http://www.posit.co/>
- Prugnolle, F., & de Meeus, T. (2002). Inferring sex-biased dispersal from population genetic tools: A review. *Heredity*, 88(3), 161–165. <https://doi.org/10.1038/sj.hdy.6800060>
- QIAGEN. (2020). *DNeasy Blood and Tissue Handbook* (HB-2061-003). <https://www.bing.com/search?q=HB-2061-003&cvid=bd6f2dd2e1ed4e528320af5bce06e6cc&aqs=edge..69i57j69i11004.1708j0j1&FORM=ANAB01&PC=HCTS>
- R Core Team. (2023). *R: A Language and Environment for Statistical Computing* [Computer software]. R Foundation for Statistical Computing. <https://www.R-project.org/>
- Ramos-Onsins, S. E., & Rozas, J. (2002). Statistical Properties of New Neutrality Tests Against Population Growth. *Molecular Biology and Evolution*, 19(12), 2092–2100. <https://doi.org/10.1093/oxfordjournals.molbev.a004034>
- Richards, V. P., Henning, M., Witzell, W., & Shivji, M. S. (2009a). *FJ812179 Aetobatus narinari haplotype Hawaii2 internal transcribed spacer 2, partial sequence (225728932; FJ812179)* [Dataset]. NCBI Nucleotide Database. <http://www.ncbi.nlm.nih.gov/nuccore/FJ812179.1>

- Richards, V. P., Henning, M., Witzell, W., & Shivji, M. S. (2009b). *FJ812206 Aetobatus flagellum internal transcribed spacer 2, partial sequence (225729094; FJ812206)* [Dataset]. NCBI Nucleotide Database. <http://www.ncbi.nlm.nih.gov/nuccore/FJ812206.1>
- Richards, V. P., Henning, M., Witzell, W., & Shivji, M. S. (2009c). Species Delineation and Evolutionary History of the Globally Distributed Spotted Eagle Ray (*Aetobatus narinari*). *Journal of Heredity*, *100*(3), 273–283. <https://doi.org/10.1093/jhered/esp005>
- Roycroft, E. J., Le Port, A., & Lavery, S. D. (2019). Population structure and male-biased dispersal in the short-tail stingray *Bathytoshia brevicaudata* (Myliobatoidei: Dasyatidae). *Conservation Genetics*, *20*(4), 717–728. <https://doi.org/10.1007/s10592-019-01167-3>
- Salazar P, S., & Bustamante, R. H. (2003). *Effects of the 1997-1998 El Niño on population size and diet of the Galápagos sea lion (Zalophus wollebaeki)*. <https://www.sidalc.net/search/Record/dig-aquadocs-1834-25262/Description>
- Sales, J. B. L., de Oliveira, C. N., dos Santos, W. C. R., Rotundo, M. M., Ferreira, Y., Ready, J., Sampaio, I., Oliveira, C., Cruz, V. P., & Lara-Mendoza, R. E. (2019). Phylogeography of eagle rays of the genus *Aetobatus*: *Aetobatus narinari* is restricted to the continental western Atlantic Ocean. *Hydrobiologia*, *836*(1), 169–183.
- Sales, J. B. L., Oliveira, C. N., Cruz, V. P., Lara-Mendoza, R. E., & Rodrigues-Filho, L. F. S. (2016). *FJ812188 Aetobatus narinari haplotype Hawaii2 cytochrome b (cytb) gene, partial cds; mitochondrial (225728944; FJ812188)* [Dataset]. NCBI Nucleotide Database. <http://www.ncbi.nlm.nih.gov/nuccore/FJ812188.1>
- Sales, J. B. L., Oliveira, C. N., Santos, W. C., Rotundo, M. M., Ferreira, Y., Sampaio, I., Oliveira, C., Cruz, V. P., Lara-Mendoza, R. E., & Rodrigues-Filho, L. F. S. (2019a). *MK340528 Aetobatus narinari voucher Anari604 cytochrome b (cytb) gene, partial cds;*

- mitochondrial* (1708630605; MK340528) [Dataset]. NCBI Nucleotide Database.
<http://www.ncbi.nlm.nih.gov/nuccore/MK340548.1>
- Sales, J. B. L., Oliveira, C. N., Santos, W. C., Rotundo, M. M., Ferreira, Y., Sampaio, I.,
Oliveira, C., Cruz, V. P., Lara-Mendoza, R. E., & Rodrigues-Filho, L. F. S. (2019b).
MK340548 Aetobatus narinari voucher Anari263 cytochrome b (cytb) gene, partial cds;
mitochondrial (1708630605; MK340548) [Dataset]. NCBI Nucleotide Database.
<http://www.ncbi.nlm.nih.gov/nuccore/MK340548.1>
- Sales, J. B. L., Oliveira, C. N., Santos, W. C., Rotundo, M. M., Ferreira, Y., Sampaio, I.,
Oliveira, C., Cruz, V. P., Lara-Mendoza, R. E., & Rodrigues-Filho, L. F. S. (2019c).
MK340549 Aetobatus narinari voucher Anari604 internal transcribed spacer 2, partial
sequence (1708630607; MK340549) [Dataset]. NCBI Nucleotide Database.
<http://www.ncbi.nlm.nih.gov/nuccore/MK340549.1>
- Sales, J. B. L., Oliveira, C. N., Santos, W. C., Rotundo, M. M., Ferreira, Y., Sampaio, I.,
Oliveira, C., Cruz, V. P., Lara-Mendoza, R. E., & Rodrigues-Filho, L. F. S. (2019d).
MK340564 Aetobatus narinari voucher Anari892 internal transcribed spacer 2, partial
sequence (1708630622; MK340564) [Dataset]. NCBI Nucleotide Database.
<http://www.ncbi.nlm.nih.gov/nuccore/MK340564.1>
- Schliep, K., Jombart, T., Kamvar, Z. N., Archer, E., & Harris, R. (2020). *apex: Phylogenetic*
Methods for Multiple Gene Data. <https://CRAN.R-project.org/package=apex>
- Silliman, K., Indorf, J., Knowlton, N., Browne, W., & Hurt, C. (2022). *Base-substitution*
mutation rate across the nuclear genome of Alpheus snapping shrimp and the timing of
isolation by the Isthmus of Panama (Version 4, p. 161764303 bytes) [Dataset]. Dryad.
<https://doi.org/10.5061/DRYAD.QNK98SFGS>

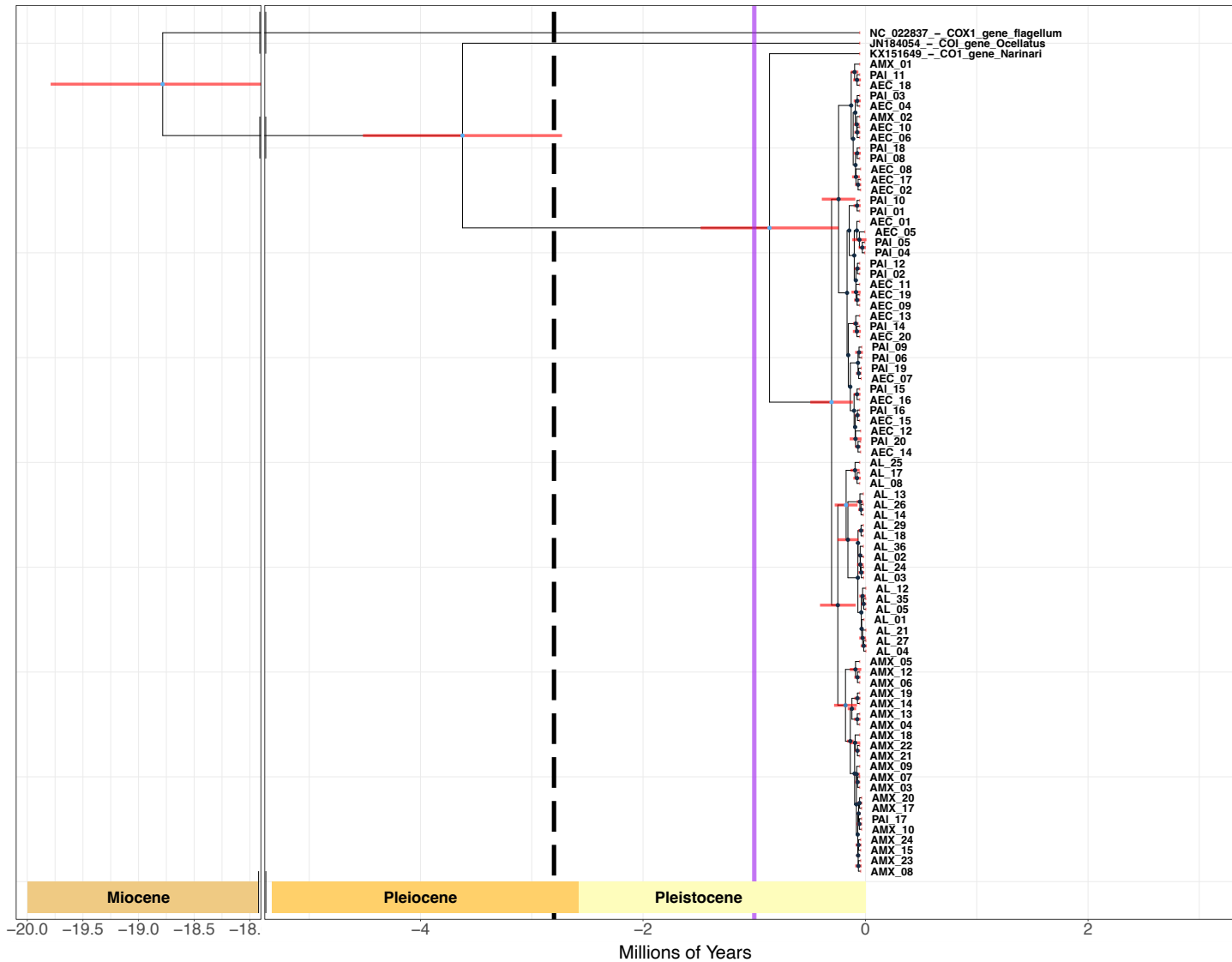
- Slatkin, M. (1987). Gene Flow and the Geographic Structure of Natural Populations. *Science*, 236(4803), 787–792. <https://doi.org/10.1126/science.3576198>
- Sokal, R. R., & Wartenberg, D. E. (1983). A test of spatial autocorrelation analysis using an isolation-by-distance model. *Genetics*, 105(1), 219–237.
- Steinfartz, S., Glaberman, S., Lanterbecq, D., Marquez, C., Rassmann, K., & Caccone, A. (2007). Genetic impact of a severe El Niño event on Galápagos marine iguanas (*Amblyrhynchus cristatus*). *PLoS One*, 2(12), e1285.
- Stevens, J. (2000). The effects of fishing on sharks, rays, and chimaeras (chondrichthyans), and the implications for marine ecosystems. *ICES Journal of Marine Science*, 57(3), 476–494. <https://doi.org/10.1006/jmsc.2000.0724>
- Trillmich, F., & Limberger, D. (1985). Drastic effects of El Niño on Galapagos pinnipeds. *Oecologia*, 67, 19–22.
- Valle, C. A., Cruz, F., Cruz, J. B., Merlen, G., & Coulter, M. C. (1987). The impact of the 1982–1983 El Niño-Southern Oscillation on seabirds in the Galapagos Islands, Ecuador. *Journal of Geophysical Research: Oceans*, 92(C13), 14437–14444. <https://doi.org/10.1029/JC092iC13p14437>
- Warnes, G. R., Bolker, B., Bonebakker, L., Gentleman, R., Huber, W., Liaw, A., Lumley, T., Maechler, M., Magnusson, A., Moeller, S., Schwartz, M., & Venables, B. (2022). *gplots: Various R Programming Tools for Plotting Data*. <https://CRAN.R-project.org/package=gplots>
- White, W. T., Corrigan, S., Yang, L., Henderson, A. C., Bazinet, A. L., Swofford, D. L., & Naylor, G. J. P. (2018). *KX151649 Aetobatus narinari isolate GN5677 mitochondrion*,

- partial genome* (1090894748; KX151649) [Dataset]. NCBI Nucleotide Database.
<http://www.ncbi.nlm.nih.gov/nuccore/KX151649.1>
- White, W. T., Last, P. R., Naylor, G. J. P., Jensen, K., & Caira, J. N. (2010). *Clarification of Aetobatus ocellatus (Kuhl, 1823) as a valid species, and a comparison with Aetobatus narinari (Euphrasen, 1790) (Rajiformes: Myliobatidae)* (By P. R. Last, W. T. White, & J. J. Pogonoski; pp. 141–146). CSIRO Marine & Atmospheric Research.
- White, W. T., & Naylor, G. J. P. (2016). Resurrection of the family Aetobatidae (Myliobatiformes) for the pelagic eagle rays, genus *Aetobatus*. *Zootaxa*, 4139(3), 435.
<https://doi.org/10.11646/zootaxa.4139.3.10>
- Winter, D. J. (2012). mmod: An R library for the calculation of population differentiation statistics. *Molecular Ecology Resources*.
- Yang, B., Zhang, J., Ding, M., & Zhang, B. (2023). *NC_022837 Aetobatus flagellum strain 09A06 mitochondrion, complete genome* (558603467; Complete Genome NC_022837). NCBI Nucleotide Database. http://www.ncbi.nlm.nih.gov/nuccore/NC_022837.1
- Yokota, L., & Lessa, R. P. (2006). A nursery area for sharks and rays in Northeastern Brazil. *Environmental Biology of Fishes*, 75, 349–360.

SUPPLEMENTARY MATERIALS AND INFORMATION

Supplementary table 1: List of accessions used for Bayesian Phylogeny outgroups and calibration nodes

Marker	Accession	Region	Species	Citation
CYTB	MK340528	México	<i>A. narinari</i>	(Sales, Oliveira, et al., 2019a)
CYTB	MK340548	Brazil	<i>A. narinari</i>	(Sales, Oliveira, et al., 2019b)
CYTB	FJ812188	Hawaii	<i>A. narinari</i>	(Sales et al., 2016)
ITS2	FJ812206	N/A	<i>A. flagellum</i>	(Richards et al., 2009b)
ITS2	FJ812179	Hawaii	<i>A. narinari</i>	(Richards et al., 2009a)
ITS2	MK340564	Brazil	<i>A. narinari</i>	(Sales, Oliveira, et al., 2019d)
ITS2	MK340549	México	<i>A. narinari</i>	(Sales, Oliveira, et al., 2019c)
Mitogenome	NC_022837	N/A	<i>A. flagellum</i>	(Yang et al., 2023)
Mitogenome	JN184054	N/A	<i>A. ocellatus</i>	(Aschliman et al., 2012)
Mitogenome	KX151649	Florida	<i>A. narinari</i>	(White et al., 2018)



Supplementary figure 1: Bayesia Tree of COI sequences

Supplementary figures 1, 2, 3, and 4 depict a most recent common ancestor calibrated Bayesian phylogeny for sequences for the COI, CYTB and ITS loci. The dots at each node are colored according to their resolution's posterior probability, lighter tones of blue signify a high posterior probability and a reliable resolution. The red horizontal bars over each node represent the 95% Highest Posterior Density on which each node could land in the temporal scale. The dotted vertical line represents the estimated timing for the formation of the Panamá Isthmus, and the vertical lilac line represents the intensification of El Niño Southern Oscillation (ENSO) events.

COI phylogeny

The same pattern can be observed in the tree built from the COI alignment in Figure 5. However, the divergence time between the Eastern Tropical Pacific samples, and the *A. narinari* accession from Florida is much more recent, by about 1.5 million years (Figure 5). The 95 % Highest Posterior Density (HPD) for this node is quite large, spanning close to one million years. Similarly, the divergence time between our samples is more recent, estimated to have occurred around 300,000 years ago. In this tree, the nodes are not as geographically distinct as in the concatenated tree in figure 4. Furthermore, the posterior probability for all the internal nodes is quite low, ranging from 0 to 0.5.

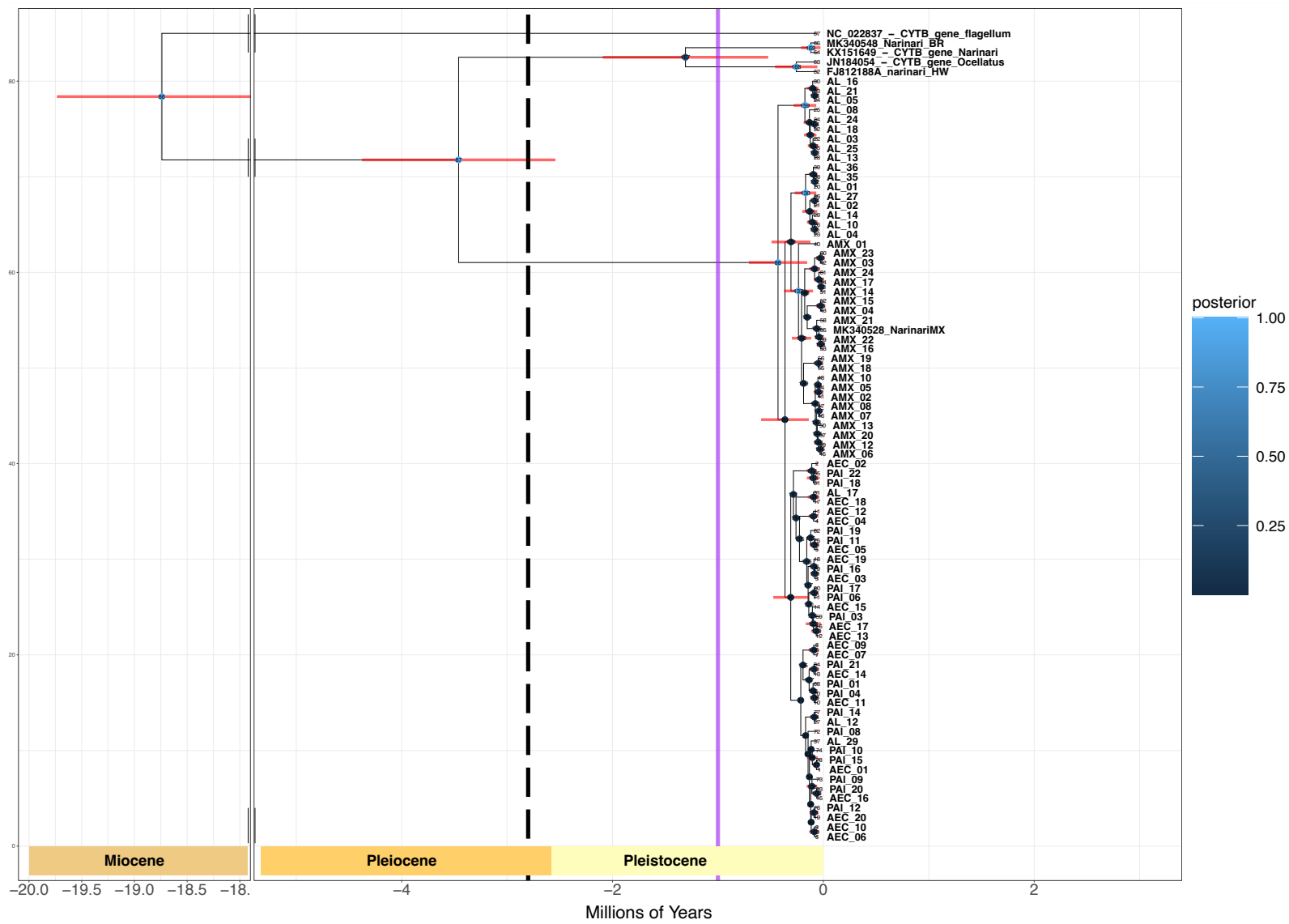
CYTB

The tree built using the Cytb sequences showed vastly different divergence patterns between our sequences and other species in the *Aetobatus* genus. We can see that the divergence time between our sequences and those from *A. narinari* accessions KX151649 and MK340548, from Florida and Brazil respectively, go back 3.5 million years ago to the Pleistocene, **before** the formation of the Panama Isthmus. In this tree, the accessions from the *A. ocellatus* sequences from the Western Pacific, specifically accessions, JN184054 and FJ812188, diverged from our sequences in the Eastern Tropical Pacific approximately 3.5 million years ago. This divergence is dated in our tree 1.3 million years earlier than the divergence of these Western Pacific sequences from the Atlantic eagle rays. One sequence obtained from NCBI, accession MK3405528, corresponding to an individual collected in Mexico was placed in the same branch as our Mexican samples.

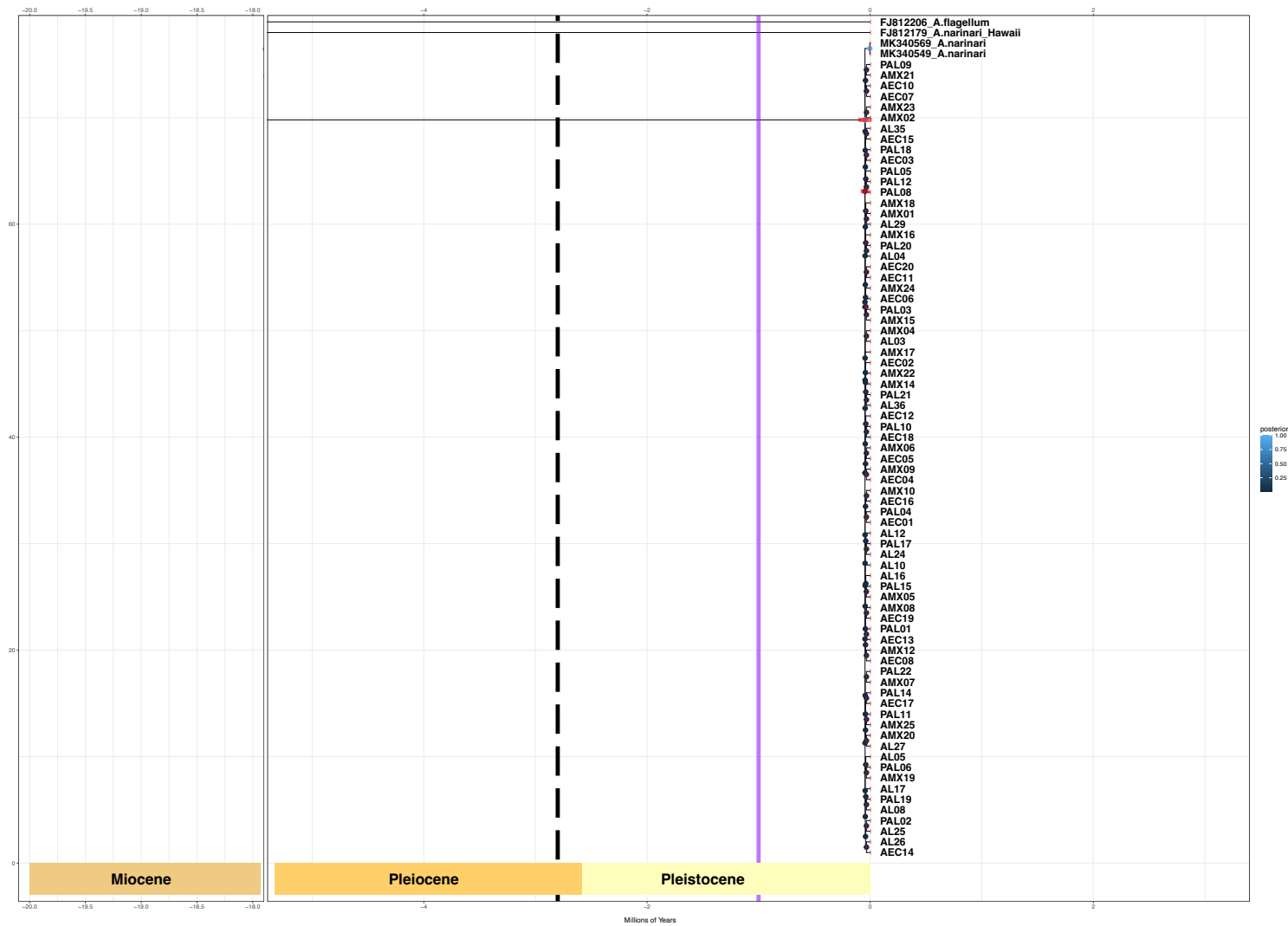
The divergence time between our sequences (within *A. laticeps* from the ETP) was similar to the results we found in the concatenated tree and the COI tree, with divergence time estimated at about 500 thousand years ago, with a very high posterior probability. However, unlike the concatenated tree, the nodes arising from this divergence did not correspond to the four regions we sampled (nodes 159 and 130 in Supplementary Figure 2). Both nodes exclusively contain individuals from Costa Rica, however where node 159 directly splits from the parent node all our sequences (node 88), node 130 branches-off from node 129, which also branches into nodes that contain individuals from Mexico.

ITS2

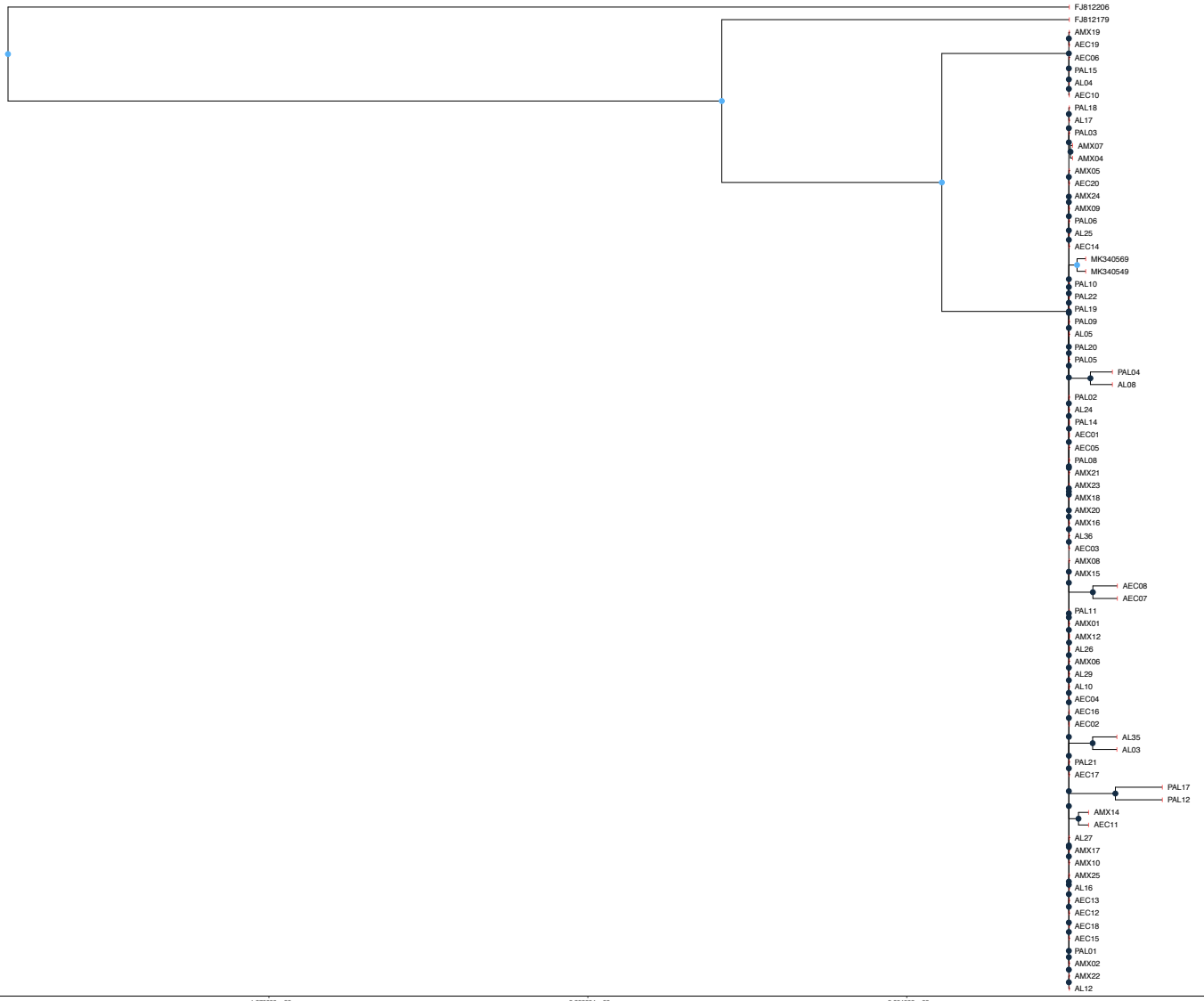
The ITS2 tree phylogeny showed no discernible branching patterns, both between our sequences and with accessions MK340569 and MK340549 (Figures 7 and 8). However, sequences from *A. flagellum*, the most basal lineage in the *Aetobatus* genus, were observed in a in a different branch separated from our sequences for more than 15 million years. The sequence from accession FJ81279 pertaining to an eagle ray sampled in Hawaii also differed significantly from our sequences, going back more than 10 million years (Figure 7).



Supplementary figure 2. Bayesian Tree of CYTB sequences



Supplementary figure 3. Bayesian Tree of Time Calibrated ITS2 Sequences



Supplementary figure 4. Bayesian Tree of Time Un-calibrated ITS2 Sequences